Microbiology and Infectious Disease

A Novel Rapid Host Cell Entry Pathway Determines Intracellular Fate of *Staphylococcus aureus*

Reviewed Preprint
v1 • November 29, 2024
Not revised

Marcel Rühling, Fabio Schmelz, Kim Ulbrich, Julia Wolf, Maximilian Pfefferle, Adriana Moldovan, Nadine Knoch, Andreas Iwanowitsch, Christian Kappe, Kerstin Paprotka, Christoph Arenz, Martin J Fraunholz

Chair of Microbiology, Julius-Maximilians-University Würzburg, Würzburg, Germany • Institut for Chemistry, Humboldt Universität zu Berlin, Berlin, Germany

eLife Assessment

This **valuable** study proposes a novel rapid-entry mechanism of S. aureus that involves the rapid release of calcium from lysosomes. The strength of the paper lies in a very interesting hypothesis; what diminishes enthusiasm is the lack of appropriate methodology, thus making the study **incomplete**. The methods used are deficient: they are largely reliant on the use of chemical inhibitors and do not adequately support the conclusions.

https://doi.org/10.7554/eLife.102810.1.sa3

Abstract

Staphylococcus aureus is an opportunistic pathogen causing severe diseases. Recently, *S. aureus* was recognized as intracellular pathogen with the intracellular niche promoting immune evasion and antibiotic resistance. We identified an alternative mechanism governing cellular uptake of *S. aureus* which relies on lysosomal Ca^{2+}, lysosomal exocytosis and occurs concurrently to other well-known entry pathways within the same host cell population. This internalization pathway is rapid and active within only few minutes after bacterial contact with host cells. Compared to slow bacterial internalization, the rapid pathway demonstrates altered phagosomal maturation as well as translocation of the pathogen to the host cytosol and ultimately results in different rates of intracellular bacterial replication and host cell death. We show that these alternative infection outcomes are caused by the mode of bacterial uptake.

Introduction

The most abundant sphingolipid, sphingomyelin (SM), resides in the extracellular leaflet of the plasma membrane and hence is exposed to the environment (1, 2). SM is a substrate for sphingomyelinases (SMases) that cleave off the phosphocholine head group to produce the non-

polar ceramide. Acid sphingomyelinase (ASM) is a lysosomal enzyme involved in recycling of SM (3, 4) and is linked to infectious diseases, where it was shown to be involved in cellular uptake of several human pathogens (5–11).

Staphylococcus aureus is a Gram-positive human commensal that asymptomatically colonizes about one third of the human population (12). It is an opportunistic pathogen causing diseases ranging from soft tissue and skin infections (13) to lethal diseases (14, 15). *S. aureus* is notorious for acquiring antibiotic resistances thereby causing >100,000 annual deaths (16). *S. aureus* possesses intracellular virulence strategies (17, 18) that contribute to antibiotic resistance (19, 20) and immune evasion (21). Internalization of *S. aureus* by host cells is mediated by several adhesins on the staphylococcal surface that bind a plethora of receptors on the host cell plasma membrane (5, 22–32). For instance, staphylococcal fibronectin-binding proteins that form fibronectin bridges to $\alpha_5\beta_1$ integrins on host cells to initiate internalization (22) or clumping factor B which can interact with the host receptor annexin A2 (25).

After internalization, *S. aureus* resides within a phagosome-like compartment that matures by acquiring proteins associated with early and then late endosomes as well as lysosomes (33–35). In epithelial and endothelial cells, the bacteria translocate to the host cytosol ("phagosomal escape") where they replicate and cause host cell death (33, 36–38).

The mechanism by which pathogens enter their host cells has been suggested to dictate the outcome of infections (39–42). For instance, phagosomes formed during natural internalization of *Brucella arbortus* by macrophages possessed different characteristics compared to phagosomes that were artificially generated by phorbol myristate acetate (42). The protozoic parasite *Toxoplasma gondii* invades its host cells by a proactive mechanism. Phagosomes generated during active invasion differed from those that were generated during Fc receptor-mediated uptake of antibody-coated parasites (41). Since previous observation connecting host cell entry and intracellular fate of pathogens were based on artificial induction of internalization, it is unclear whether pathogens can enter host cells within the same population via different naturally occurring mechanisms and if the entry route has a direct influence on the outcome of an intracellular infection.

Here, we describe the internalization of *S. aureus* by tissue cells via a rapid pathway taking place within minutes after contact between bacteria and host cell surface. This pathway requires nicotinic acid adenosine dinucleotide phosphate (NAADP)-dependent mobilization of lysosomal Ca^{2+}, followed by lysosomal exocytosis and thereby release of ASM. Since the rapid uptake is concurrent to previously known internalization pathways, it probably has been missed due to long infection times used in traditional infection protocols (e.g., (22, 25, 29, 30)).

S. aureus bacteria, which enter host cells of the same cell population via the rapid pathway, cause a distinct infection outcome with altered phagosome maturation, bacterial translocation to host cytosol and eventually host cell death when compared to bacteria that enter host cells at later time points during infection. Thus, the outcome of an infection is decided at the single cell level during bacterial uptake at the host plasma membrane. Bacteria-containing phagosomes that were formed by the ASM-dependent rapid uptake pathway are delayed in their maturation and the bacteria do not escape these organelles efficiently, hence demonstrating a direct link between concurrently active modes of bacterial uptake and the resulting outcomes of intracellular *S. aureus* infection.

Results

S. aureus triggers lysosomal Ca^{2+} mobilization for host cell invasion

We previously identified that internalization of *S. aureus* by host cells is associated with cellular Ca^{2+} signaling (43). To delineate the role of Ca^{2+} in this process mechanistically, we pretreated human microvascular endothelial cells (HuLEC) with the calcium ionophore ionomycin, which reduced bacterial invasion efficiency dose-dependently (**Figure 1**, A), at concentrations neither affecting bacterial (**Supp. Figure 1**, A, B) nor host cell viability (**Supp. Figure 1**, C).

Since focal adhesions constitute major cellular entry sites for *S. aureus* and the Ca^{2+}-activated transient receptor potential ion channel 4 (TRPM4) is located therein, we inhibited TRPM4 with 9-Phenantrol. 9-Phenantrol reduced invasion efficiency (**Figure 1**, B), but was not bactericidal (**Supp. Figure 1**, D). Further, treatment of HuLEC (**Figure 1**, C) or HeLa (**Supp. Figure 1**, E) with the Ca^{2+} chelator BAPTA-AM (44) led to reduction of *S. aureus* invasion in a concentration-dependent manner.

The pore-forming staphylococcal α-toxin has been shown to mediate Ca^{2+} influx into host cells (45). However, *S. aureus* invasion was independent of toxin production in HeLa and only slightly reduced in endothelial cells (**Supp. Figure 1**, F). Consequently, omission of Ca^{2+} from the cell culture medium did not affect internalization of bacteria, indicating that invasion is not dependent on Ca^{2+} influx (**Figure 1**, C).

Since intracellular Ca^{2+} stores can serve as alternative source of Ca^{2+}, we next blocked Ca^{2+} liberation from the ER using 2-APB (46) or 8-Bromo-cyclic ADP ribose (8-Bromo-cADPR; (47)) and from lysosomes using *trans*-Ned19 (48) in HuLEC (**Figure 1**, D) or HeLa (Supp. Figure 1, G, H) at concentrations not affecting bacterial viability (**Supp. Figure 1**, I and J). Interference with lysosomal, but not ER Ca^{2+} release reduced internalization of *S. aureus*.

Ned19 antagonizes NAADP, a second messenger that mediates opening of two pore channels (TPCs) which transport Ca^{2+} from the endo-lysosomal compartment into the cytosol (48). Hence, a HeLa cell pool depleted of TPC1 (Supp. Figure 1, K) substantially reduced invasion when compared to unmodified HeLa cells. This was particularly pronounced after a 10 min infection pulse, suggesting that Ca^{2+}-dependent invasion is important early in infection (**Figure 1**, E).

CD38 is a well-known producer of NAADP in immune cells (49–51). Thus, we tested *S. aureus* invasion in HeLa cells treated with the specific CD38 inhibitor 78c, even though expression of CD38 in these cells is predicted to be very low (*proteinatlas.org*). We observed no effect on *S. aureus* invasion by CD38 inhibition (Supp. Figure 1, L). An alternative NAADP producer, with higher expression in our infection model, is *Sterile Alpha and TIR Motif Containing 1* [SARM1, (52)]. We measured a slightly decreased invasion efficiency 10 min p.i. in a cell pool lacking SARM1 when compared to WT cells (**Figure 1**, F; **Supp. Figure 1**, M), suggesting that SARM1 might be enrolled in NAADP production during internalization of *S. aureus* by host cells.

Altogether, our findings support the important role of lysosomal Ca^{2+} mobilization in *S. aureus* invasion as particularly required early in infection.

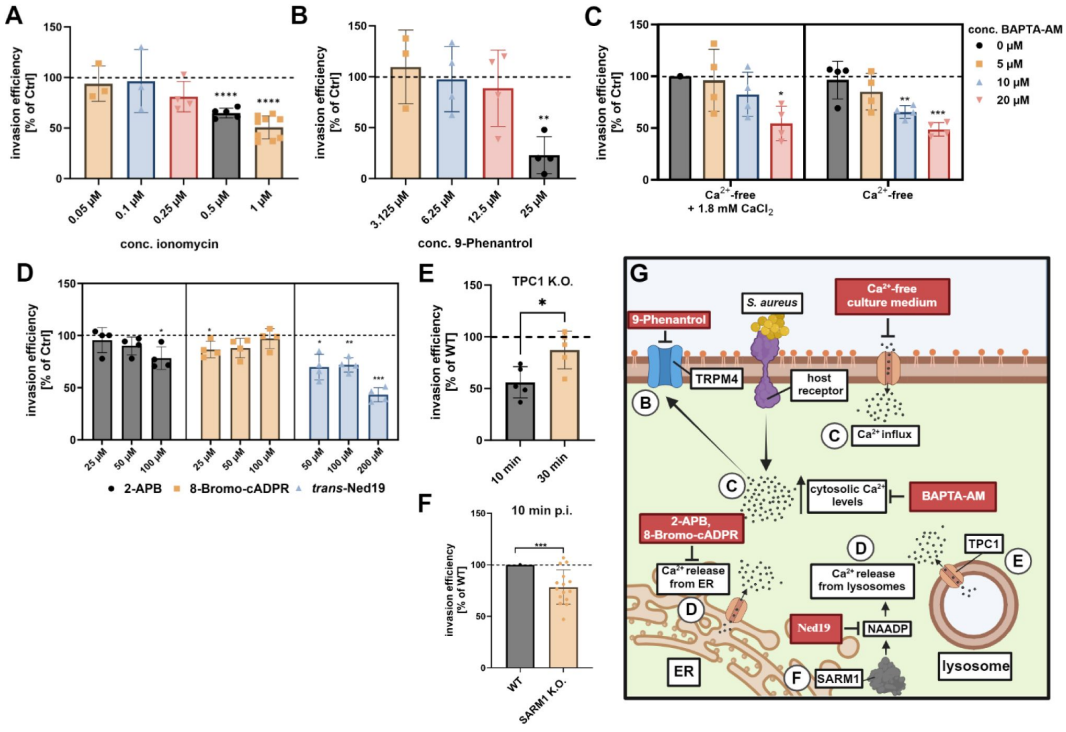

Figure 1

S. aureus invasion is dependent on Ca^{2+} liberation from lysosomal stores and lysosomal exocytosis.

Treatment with Ionomycin (A, n≥3), 9-Phenantrol (B, n≥3), BAPTA-AM (C, n≥4), *trans*-Ned19 (D, n≥4), but not 2-APB and 8-Bromo-cADPR (D, n≥4) reduce *S. aureus* internalization by host cells in a TPC1 dependent fashion (E, n≥5). HuLEC (A, C, D, F), HeLa WT (B), HeLa TPC1 K.O. (E) or HeLa SARM1 K.O. (F) cells were treated with the respective substance and were subsequently infected with *S. aureus* JE2 for 30 min if not indicated otherwise. Extracellular bacteria were removed by lysostaphin, and the number of intracellular bacteria was determined by CFU counting. Results were normalized to untreated controls to obtain invasion efficiency (in percent of control). (F) scheme of host cell Ca^{2+} signaling and interfering agents. Statistics: one sample t-test (A-D, F), unpaired Student's t-test (E). Bars represent means ± SD. *p≤0.05, **p≤0.01, ***p≤0.001, ****p≤0.0001.

Created with *BioRender.com/k99z626*.

Rapid S. aureus invasion requires lysosomal exocytosis, ASM and its substrate sphingomyelin on the host cell surface

Ionomycin treatment results in lysosomal exocytosis, a Ca^{2+}-dependent process in which lysosomes release their content to the extracellular space (45, 53). Hence, we treated host cells with Vacuolin-1, an inhibitor blocking this process (54), which reduced invasion efficiency in HuLEC (**Figure 2**, A) and HeLa cells (**Supp. Figure 2**, A), while not affecting survival of the bacteria (**Supp. Figure 2**, B).

Synaptotagmin 7 (Syt7) is known to support fusion of lysosomes with the plasma membrane in a Ca^{2+}-dependent manner (55). Accordingly, Syt7-depleted HeLa cells demonstrated lower bacterial invasion (**Figure 2**, B). As already observed for TPC1 (**Figure 1**, E), this was most pronounced early in infection further supporting our hypothesis that lysosomal exocytosis is important for rapid invasion events.

Lysosomal exocytosis results in release of ASM (45, 56). Therefore, prior to infection, the cells were exposed to amitriptyline, a functional inhibitor of ASM (FIASMA), or a competitive inhibitor [ARC39, (57)] at concentrations not affecting bacterial survival (**Supp. Figure 2**, C, D). While invasion in HuLEC, human umbilical vein endothelial cells (HuVEC) and HeLa was sensitive to both inhibitors, invasion in 16HBE14o$^-$ and EA.hy926 was not or only marginally affected (**Figure 2**, C). We excluded that differences among cell lines arose from differential ASM activity or sensitivity to the inhibitors by monitoring enzymatic activity [**Supp. Figure 2**, E; (58) and **Supp. Figure 2**, F; (59)].

Next, we treated HuLEC with 10 µM ARC39 or 0.5 µM PCK310, a fast-acting ASM inhibitor. Already after 1h preincubation, PCK310 reduced invasion of *S. aureus*, whereas ARC39 required overnight treatment for a similar reduction (**Figure 2**, D). Taken together, these results show that ASM is involved in *S. aureus* invasion of host cells.

We removed SM, the substrate of ASM, from plasma membranes of HuLEC (**Figure 2**, E) and HeLa (**Supp. Figure 2**, G) by pretreatment with the bacterial SMase β-toxin. Most human pathogenic *S. aureus* strains including JE2, the strain we use in the present study, do not produce β-toxin, due to a genomic integration of a prophage (60). SMase pretreatment reduced invasion efficiency in a concentration-dependent manner in both cell lines. 10 ng/ml β-toxin were sufficient to decrease invasion to 34.37 ± 6.24% of that measured in untreated control cells. Interestingly, a 250-fold higher concentration did not lead to further reduction. In line with our previous experiments, this suggests that multiple *S. aureus* invasion pathways exist within the same host cell population, of which at least one requires SM and its enzymatic breakdown on the plasma membrane.

Next, we infected wild-type as well as the TPC1 or Syt7 K.O. cells with *S. aureus* in presence (but without pretreatment) of 100 ng/ml β-toxin and determined the number of intracellular bacteria after 10 min (**Figure 2**, F). Presence of β-toxin in the culture medium completely rescued the invasion defect of the K.O. cells. This indicates that reduced bacterial internalization in absence of TPC1 and Syt7 results from a lack in ASM delivery to the cell surface by Ca^{2+}-dependent lysosomal exocytosis.

ASM- and Ca^{2+}-mediated invasion is rapid

To study the role of SM in *S. aureus* uptake kinetics, we incubated HuLEC with fluorescent sphingolipid analogs and recorded *S. aureus* infection by time lapse imaging [**Figure 3**, A; Supp. Video 1; **Supp. Figure 3**; Supp. Video 2; (59)]. We observed that the bacteria were rapidly engulfed by SM-containing membrane compartments. While association of bacteria with BODIPY-

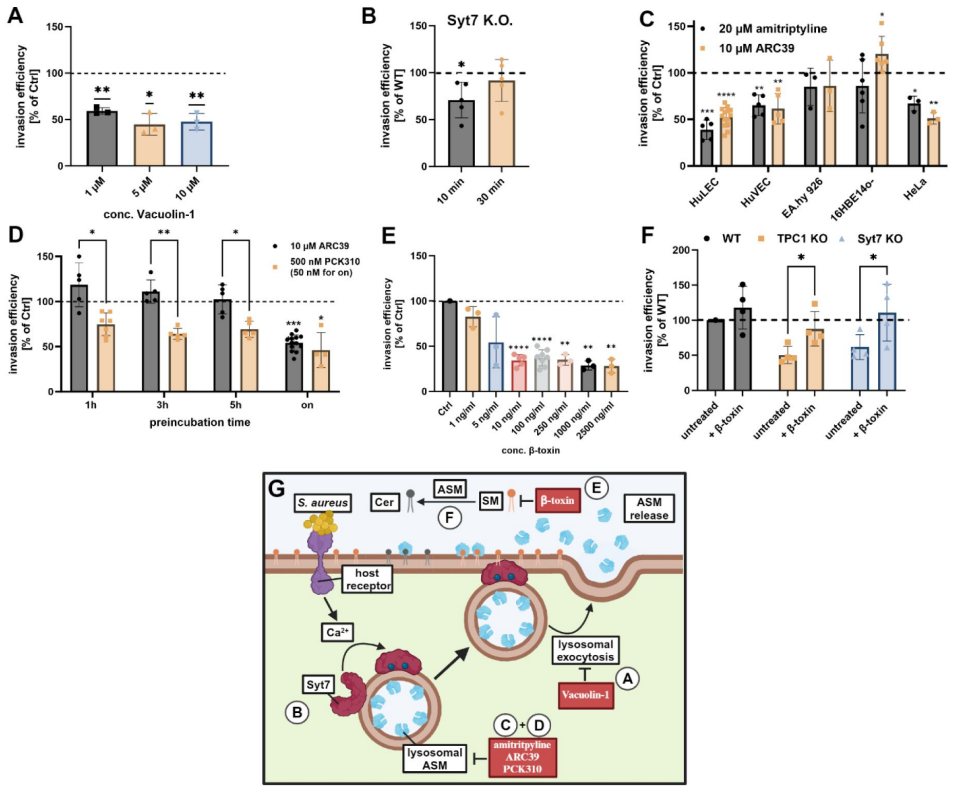

Figure 2

S. aureus invasion requires lysosomal exocytosis, ASM and plasma membrane sphingomyelin.

(A, B) *S. aureus* invasion requires Syt7-dependent lysosomal exocytosis. HuLEC were treated with the lysosomal exocytosis inhibitor Vacuolin-1 and invasion efficiency of *S. aureus* was determined 30 min p.i. (A, n=3). Invasion efficiency of *S. aureus* JE2 was determined in HeLa Syt7 K.O. cells 10 min and 30 min p.i. (B, n=5; data normalized to HeLa WT). **(C, D)** *S. aureus* internalization is dependent on ASM activity in endothelial and epithelial cells. Indicated cell lines were treated with the ASM inhibitors amitriptyline or ARC39 **(C)** and invasion efficiency of *S. aureus* was determined (n≥3). (D) HuLEC were treated with PCK310 or ARC39 for the indicated periods. Subsequently, cells were infected with *S. aureus* for 30 min and invasion efficiency was determined by CFU counting (n≥4). **(E, F)** *S. aureus* invasion requires SM and SMase activity on host cell plasma membranes. HuLEC were treated with the bacterial SMase β-toxin for 75 min and were subsequently infected with *S. aureus* JE2 for 30 min (n≥3). **(F) Presence of extracellular SMase activity restores invasion defect in TPC1 and Syt7 K.O. cell lines.** HeLa wild type as well as TPC1 or Syt7 KO cell lines were infected with *S. aureus* JE2 in presence of 100 ng/ml of the bacterial SMase β-toxin and invasion efficiency 10 min p.i. was determined (n=4). In each experiment the numbers of intracellular *S. aureus* JE2 were determined by lysostaphin protection assay and CFU counting. Results obtained for the tested condition were normalized to the wildtype cell line or the mock-treated control. (**G) scheme of lysosomal exocytosis and ASM release as well as interfering agents.** Cer: ceramide, SM: sphingomyelin, ASM: acid sphingomyelinase. Statistics: one sample t-test (A-C, E), one-way ANOVA and Dunnett's multiple comparisons test (D). Two-way ANOVA and Tukey's multiple comparison (F). Bars represent means ± SD. *p≤0.05, **p≤0.01, ***p≤0.001, ****p≤0.0001.
Created with *BioRender.com/u99k818*.

FL-C12-SM increased over time during the first 30 min of infection, this was not observed for BODIPY-FL-C12-Ceramide, suggesting that *S. aureus* invasion specifically relies on interaction with SM in plasma membranes (**Figure 3**, B). Next, we determined the invasion efficiency of *S. aureus* in a time-dependent manner and blocked invasion by either ASM inhibitors, ionomycin, BAPTA-AM or β-toxin pretreatment. We found a time-dependent increase in intracellular bacteria, whereby all treatment conditions reduced bacterial invasion at every time point with the untreated control at 30 min set to 100% (**Figure 3**, C). By normalizing the data to the untreated control at the corresponding time points, we found that -with exception of β-toxin-the effect of the treatments was most pronounced early (5-10 min) after infection (**Figure 3**, D). Thus, early during infection bacteria enter the host cell predominantly in an ASM- and Ca^{2+}-dependent manner.

The mode of S. aureus invasion affects infection outcome

After invasion, *S. aureus* resides within Rab5-positive early and subsequently, in Rab7-positive late phagosomes (33). We pretreated a HeLa cell line stably expressing mCherry-Rab5 as well as YFP-Rab7 with amitriptyline and infected with *S. aureus* for different time periods and determined the proportion of bacteria that associated with Rab5 and/or Rab7 (**Figure 4**, A).

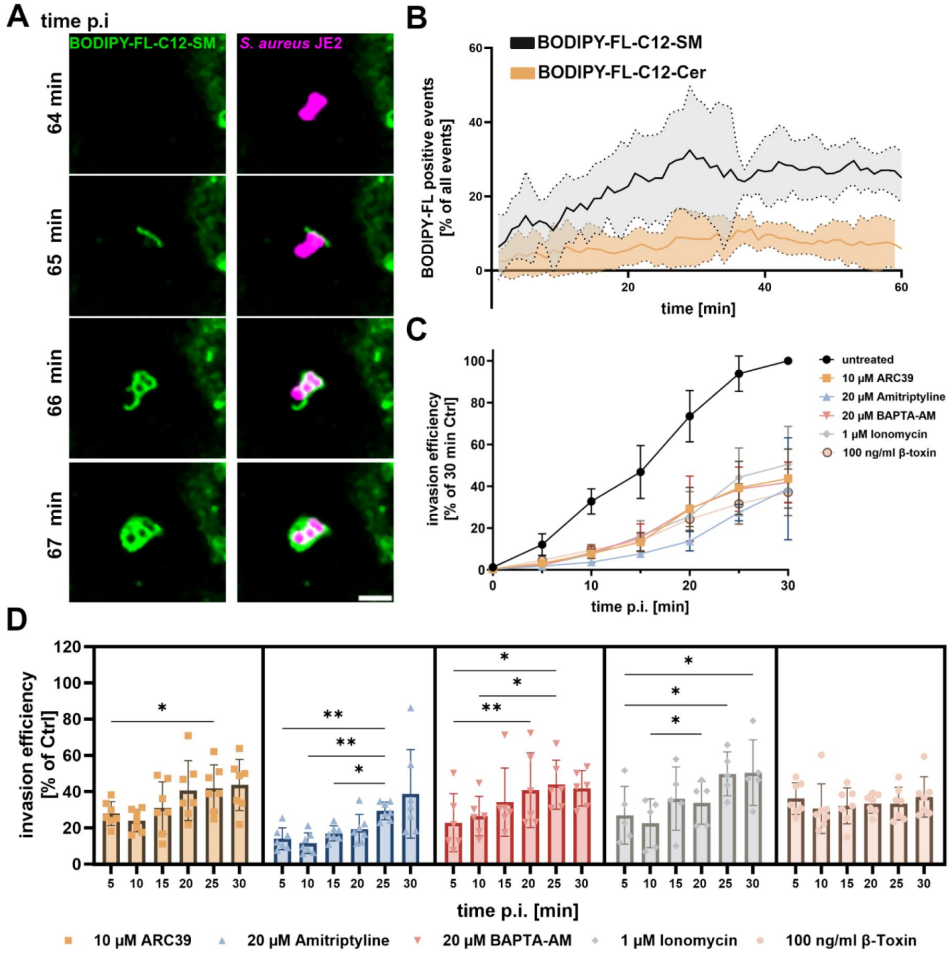

Figure 3

ASM- and Ca^{2+}-dependent uptake is rapid and predominantly mediates invasion early in infection.

(A, B) *S. aureus* associates with SM early during invasion. HuLEC were pretreated with BODIPY-FL-C12-SM or BODIPY-FL-C12-ceramide and infected with red-fluorescent *S. aureus.* Scale bar: 5 µm. Infection was monitored by live cell imaging and the proportion of bacteria that associated with the lipid analogs was quantified in each individual frame (SM: n=5, Cer: n=3). (**C, D) ASM and Ca^{2+}-dependent invasion is rapid.** HuLEC were treated with ARC39, amitriptyline, BAPTA-AM, ionomycin, or the bacterial SMase β-toxin. Then, cells were infected with *S. aureus* and the number of invaded bacteria was determined after different time periods. The results were either normalized to 30 min time point of untreated controls (C) or to the corresponding time points of the untreated controls (D). (n ≥5). Statistics: Mixed effect analysis and Tukey's multiple comparison. Graphs represent means ± SD. *p≤0.05, **p≤0.01, ***p≤0.001, ****p≤0.0001.
Created with *BioRender.com/f02t628*.

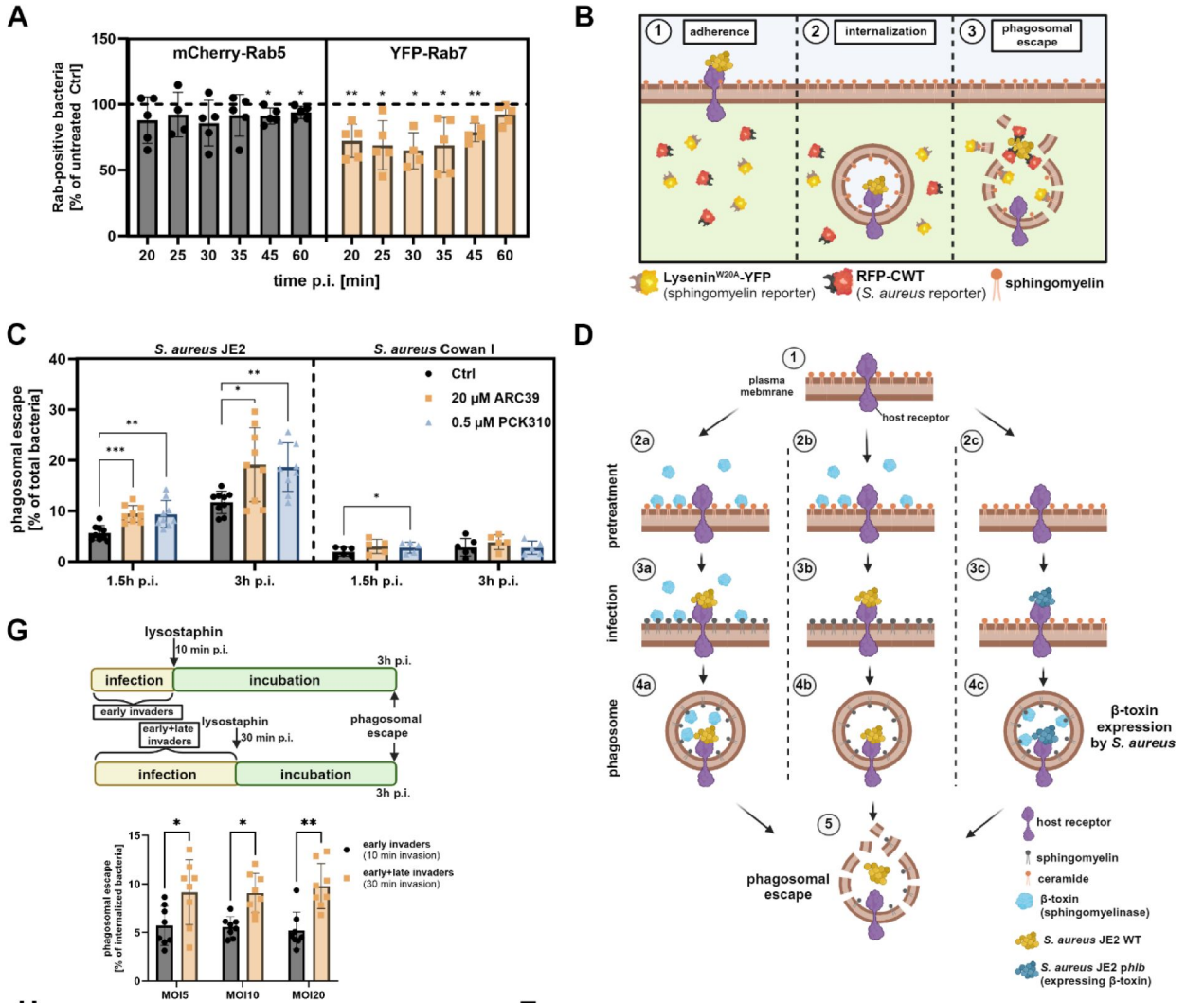
A
mCherry-Rab5
YFP-Rab7
Rab-positive bacteria [% of untreated Ctrl]
time p.i. [min]
B
1 adherence
2 internalization
3 phagosomal escape
Lysenin W20A-YFP (sphingomyelin reporter)
RFP-CWT (S. aureus reporter)
sphingomyelin
C
S. aureus JE2
S. aureus Cowan I
Ctrl
20 µM ARC39
0.5 µM PCK310
phagosomal escape [% of total bacteria]
1.5h p.i.
3h p.i.
D
plasma membrane
host receptor
pretreatment
infection
phagosome
phagosomal escape
β-toxin expression by S. aureus
host receptor
sphingomyelin
ceramide
β-toxin (sphingomyelinase)
S. aureus JE2 WT
S. aureus JE2 phlb (expressing β-toxin)
G
lysostaphin
10 min p.i.
infection
incubation
3h p.i.
early invaders
early+late invaders
30 min p.i.
phagosomal escape
phagosomal escape [% of internalized bacteria]
early invaders (10 min invasion)
early+late invaders (30 min invasion)
MOI5
MOI10
MOI20
H
S. aureus JE2 RFP
infection I
infection II
20 min p.i.
S. aureus JE2 Cerulean
E
Ctrl
β-toxin
phagosomal escape [% of internalized bacteria]
time p.i.
F
Lysenin-positive escape [% of all escape events]
time p.i.

Figure 4

The intracellular fate of *S. aureus* is determined by the pathway of cell entry.

(A) Inhibition of ASM delays formation of Rab7-positive phagosomes. HeLa cells expressing mCherry-Rab5 and YFP-Rab7 were either treated with amitriptyline or left untreated. Then, cells were infected with *S. aureus* JE2 for indicated periods. Extracellular bacteria were removed and proportion of intracellular bacteria associating with Rab5 or Rab7 was determined by CLSM. Results obtained for amitriptyline-treated samples were normalized to untreated controls (n=5). **(B) Detection of phagosomal SM and phagosomal escape by a reporter cell line expressing Lysenin^{W20A}-YFP and RFP-CWT.** After internalization, *S. aureus* resides in a phagosome preventing the recruitment of RFP-CWT to *S. aureus* cell wall and Lysenin^{W20A}-YFP to luminal SM, respectively. When the bacteria lyse the phagosomal membrane, luminal SM gets exposed to the cytosol and attracts Lysenin^{W20A}-YFP, while RFP-CWT is recruited to the staphylococcal surface. (**C) Blocking ASM-dependent internalization affects phagosomal escape.** RFP-CWT and Lysenin^{W20A}-YFP expressing HeLa were treated with PCK310, or ARC39 and infected with *S. aureus* strains JE2 or Cowan I. Thereby, β-toxin was either removed prior to infection (pretreatment only) or was present during the whole experiment (pretreatment + during infection). By CLSM, proportions of bacteria that recruited RFP-CWT (phagosomal escape) were determined (n≥3). **(D-F) Phagosomal escape depends on presence of plasma membrane SM during invasion, but not presence of SM within phagosomal membranes** HeLa RFP-CWT Lysenin^{W20A}-YFP were pretreated with β-toxin to remove surface SM (2a, 2b) or left untreated (2c). Then, cells were infected with *S. aureus* JE2 in presence (3a) or absence (3b) of β-toxin. Untreated samples (3c) were infected with *S. aureus* JE2 harboring a plasmid either encoding β-toxin and the fluorescence protein Cerulean (pCer+*hlb*) or solely Cerulean (pCer). Proportion of bacteria that recruited RFP-CWT (phagosomal escape, E) and the percentage of phagosomal escape events that additionally were positive for Lysenin^{W20A}-YFP (F) were determined at indicated time points p.i. (n=5). **(G, H) Early ASM-dependent invaders possess lower escape rates than late invaders.** HeLa cells expressing RFP-CWT were infected with indicated MOIs of *S. aureus* JE2 either for 10 min (early invaders) or 30 min (early+late invaders). Phagosomal escape rates were determined 3h p.i. (G). HeLa reporter cells expressing YFP-CWT were infected with an MOI=5 of *S. aureus* JE2 expressing a fluorescent protein (e.g. RFP) for 30 min (early+late invaders). After 20 min, the same samples were infected with *S. aureus* JE2 expressing another fluorophore (e.g. Cerulean) for 10 min (early invaders) and phagosomal escape was determined 3 h p.i. (H). Statistics: one sample t-test (A), Mixed effects analysis (REML) and Tukey's multiple comparison (C,G, H), Two-way ANOVA and Šídák's multiple comparisons test (E, F). Graphs represent means ± SD. *p≤0.05, **p≤0.01, ***p≤0.001, ****p≤0.0001.

Created with *BioRender.com/f97r445*.

While ASM inhibition marginally affected *S. aureus* association with Rab5-positive phagosomes, that with the Rab7-positive compartment was significantly reduced compared to the untreated control. This was restricted to shorter infection pulses (5-45 min) and was not observed for long infection periods (60 min). We also observed a reduced proportion of bacteria associating with Rab7-positive membranes after treatment with PCK310 or bacterial SMase. However, this was not caused by translocation of *S. aureus* to the host cytosol (**Supp. Figure 4**, A, B). Hence, phagosomes generated ASM-dependently possess different maturation dynamics when compared to phagosomes formed in an ASM-independent fashion.

Next, we measured phagosomal escape while simultaneously detecting SM content of disrupted phagosomal membranes. Therefore, we used a HeLa reporter cell line that cytosolically expresses the phagosomal escape reporter RFP-CWT (36) as well as the SM reporter Lysenin^{W20A}-YFP (61), respectively (**Figure 4**, B). Reporter gene expression in the cell line did not alter *S. aureus* invasion dynamics under different treatment conditions (**Supp. Figure 4**, C). The reporter cells were left untreated or were pre-exposed to ASM inhibitors and were infected with *S. aureus* strain JE2. In addition, *S. aureus* Cowan I, a strain known to have low escape rates, was

used for infection. The proportion of bacteria that escaped from the phagosome (**Figure 4**, C) as well as the proportion of escape events that additionally were positive for cytosolic SM (Supp. Figure 4, D) were determined 1.5 h and 3 h p.i. (see also Supp. Figure 5, A-D).

Whereas no differences for Lysenin-positive escape events were detected (**Supp. Figure 4**, D), a higher proportion of bacteria escaped from phagosomes on abrogation of ASM activity regardless of the inhibitor used (**Figure 4**, C; **Supp. Figure 4**, E). A similar increase was observed when we blocked lysosomal exocytosis by Vacuolin-1 (**Supp. Figure 4**, F).

Since blocking of ASM-dependent uptake reduced the number of intracellular bacteria but increased their phagosomal escape rates, we hypothesized that the presence of SM on the plasma membrane affects downstream events during *S. aureus* infection. To address this question, we pretreated host cells with the bacterial SMase β-toxin to block SM-dependent invasion (**Figure 4**, D; 2a, 2b) and either infected the cells in presence (3a) or after removal of the toxin (3b). β-toxin pretreatment, resulted in enhanced phagosomal escape rates of *S. aureus* JE2, independent of the presence of β-toxin during infection (**Figure 4**, E; 4a, 4b). This was not observed for infection with the non-cytotoxic Cowan I strain, indicating that removal of SM by β-toxin did not affect general phagosomal membrane stability (**Supp. Figure 4**, G). Moreover, β-toxin treatment strongly reduced recruitment of Lysenin^{W20A}, demonstrating effective removal of SM from membranes by β-toxin (**Figure 4**, F and **Supp. Figure 5**, E-J).

To investigate if removal of SM was important at the cell surface or within the phagosome, we infected the cells with an *S. aureus* JE2 strain recombinantly overexpressing β-toxin and Cerulean, or a strain solely expressing Cerulean. We did not observe increased phagosomal escape upon overexpression of β-toxin (**Figure 5**, E; 4c), although SM levels of phagosomal membranes were reduced (**Figure 5**, F) comparably to samples pretreated with β-toxin (see above). Moreover, we did not detect substantial differences in escape rates of *S. aureus* 6850, a strain naturally producing β-toxin (**Supp. Figure 4**, H), and an isogenic β-toxin mutant. By contrast, escape of *S. aureus* 6850 again was enhanced upon pretreatment with β-toxin (**Supp. Figure 4**, I) accompanied by absence of SM from phagosomal membranes (**Supp. Figure 4**, J).

Phagosomal escape of *S. aureus* thus is independent of SM levels within the infected phagosomes, but rather reflects the presence of SM and ASM at the plasma membrane during host cell entry.

To demonstrate that phagosomal escape is dependent on the pathway of cell entry, we infected reporter cells with *S. aureus* for either a 10 min (“early invaders”) or a 30 min infection pulse (“early and late invaders”). Subsequently, we determined phagosomal escape rates (**Figure 4**, H) as well as the number of invaded bacteria (**Supp. Figure 4**, K). Independent of the multiplicity of infection (MOI) used, bacteria taken up within the first 10 min demonstrated significantly lower escape rates when compared to bacteria that were cocultured with host cells for 30 min.

This was corroborated by HeLa YFP-CWT infected with *S. aureus* expressing a fluorescent protein (e.g. mRFP) for 30 min (“early and late invaders”). After 20 min, we initiated a second infection pulse for 10 min (“early invaders”) with a *S. aureus* strain expressing another fluorescence protein (e.g. Cerulean) and determined phagosomal escape rates of both bacterial recombinants (**Figure 4**, I). Again, early invaders demonstrated lower escape rates when compared to the 30 min control. This was independent of the fluorescence expressed by the strain that was used for each infection pulse.

We next monitored phagosomal escape over 10 h in cells pretreated with ASM inhibitors (**Figure 5**, A). The compounds enhanced escape rates 3 h p.i. when compared to untreated controls. In contrast, 6 h p.i. escape rates were found decreased upon ASM inhibition.

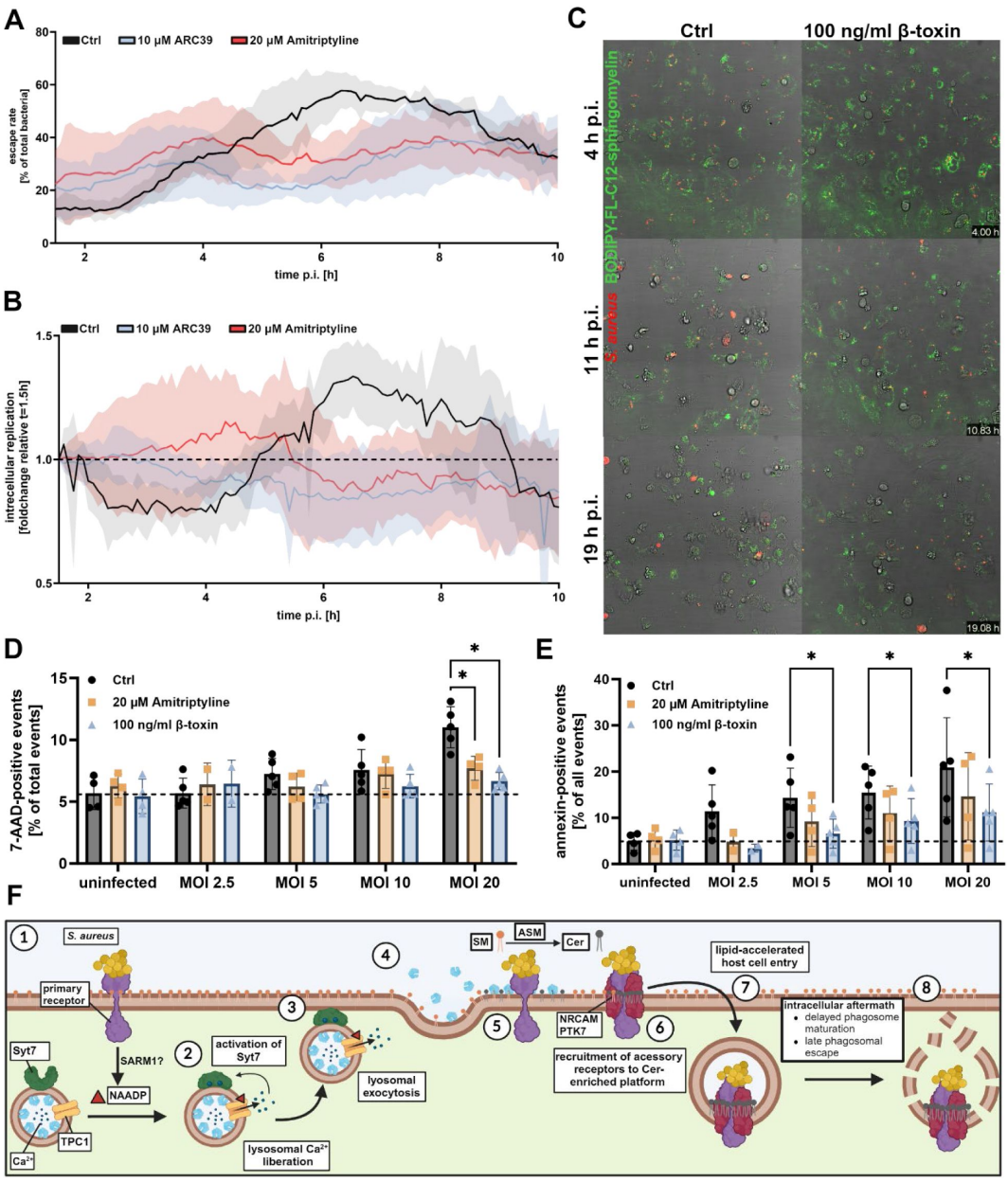

Figure 5

Blocking ASM-dependent internalization affects intracellular replication and host cell survival.

(A, B) HeLa cells expressing RFP-CWT and Lysenin^{W20A}-YFP were treated with amitriptyline or ARC39 or were left untreated (Ctrl). The cells were subsequently infected with *S. aureus* and infection was monitored for 10 h by CLSM. Proportion of escaped bacteria (A) or the intracellular replication (B) was determined (n= 5). **(C)** HuLEC were stained with BODIPY-FL-C12-SM (green), and either were pretreated with 100 ng/ml of β-toxin or were left untreated. Then, cells were infected with *S. aureus* (red) and infection was monitored by CLSM for 19 h. **(D, E)** HuLEC were treated with amitriptyline or β-toxin and subsequently infected with *S. aureus*. After 21 h, plasma membrane integrity was measured by 7-AAD staining (D), and proportion of apoptotic cells was determined by annexin V staining (E) (n=5). See also Supp. Figure 6. (F) Model: *S. aureus* interacts with an unknown primary receptor (1) that triggers production of NAADP, which in turn activates TPC1 to mediate lysosomal Ca^{2+} release and activation of Syt7 (2). Syt7-dependent lysosomal exocytosis (3) leads to release of ASM (4) and production of Cer on the plasma membrane (5) thereby resulting in the recruitment of co-receptors (6) and rapid internalization of *S. aureus* by host cells (7). Bacteria that enter the host cells via the rapid pathway experience a different intracellular fate than bacteria that entered via other pathways. Statistics: Mixed effects analysis (REML) and Tukey's multiple comparison test. Graphs represent mean ± SD. *p≤0.05.
Created with *BioRender.com/t33f620*.

Taken together, the efficiency of phagosomal escape of *S. aureus* is directly affected by the mode of cell entry, whereby the rapid SM/ASM-dependent pathway results in delayed phagosomal escape, while bacteria that entered host cells ASM-independently escape earlier during infection.

Since translocation to the host cytosol is a prerequisite for *S. aureus* replication in non-professional phagocytes, we recorded intracellular growth of *S. aureus.* In untreated controls replication started about 5 h p.i., and thus shortly after phagosomal escape (3-4 h p.i., **Figure 5**, B). By contrast, we did not observe significant bacterial replication in cells treated with ASM inhibitors (**Figure 5**, B).

We next treated HuLEC with β-toxin, stained the cells with BODIPY-FL-C12-SM and infected the cells with fluorescent *S. aureus*. Live cell imaging demonstrated that most untreated host cells died after 11 h p.i., whereas β-toxin-treated samples showed higher survival rates (**Figure 5**, C). This was also observed by cell death assays measuring i) membrane integrity (7-AAD staining, **Figure 5**, D), ii) apoptosis (Annexin V staining, **Figure 5**, E), iii) number of host cells that remained attached to the substratum (**Supp. Figure 6**, A) and iv) host cell lysis by LDH release (**Supp. Figure 6**, B).

Discussion

ASM previously has been implicated in the invasion of several viral, bacterial, and eukaryotic pathogens (5–11). However, the dynamics of ASM-mediated host cell entry, the underlying receptors as well as effects on post-invasion events are only poorly understood.

We here show that ASM is involved within minutes after the pathogen contacts host cells and is concurrent with ASM-independent uptake pathways. We demonstrate that the infection outcome of bacteria that enter the host cells via this rapid pathway is distinct from other entry mechanisms.

We observed a reduction of bacterial invasiveness upon treatment with different ASM inhibitors (**Figure 2**, C, D) or removal of the enzyme substrate SM from the plasma membrane (**Figure 2**, E) confirming that ASM activity on the host cell surface is crucial for pathogen internalization.

Release of ASM is caused by lysosomal exocytosis (56). Consequently, the inhibitor Vacuolin-1 as well as genetic ablation of Syt7, a key protein in lysosomal exocytosis (55), resulted in drastically reduced internalization of bacteria (**Figure 2**, A, B).

Elevation of cytosolic Ca^{2+} levels lead to recruitment of lysosomes to the cell surface (53). Whereas most studies implicated Ca^{2+} influx from the extracellular milieu (8, 10), we here demonstrate that *S. aureus* mainly triggers lysosomal Ca^{2+} mobilization as was shown by treatment with the inhibitor *trans*-Ned19 as well as a genetic K.O. of the endo-lysosomal Ca^{2+} channel TPC1 (**Figure 1**, D and E; **Supp. Figure 1**, G). TPCs have previously been associated with regulation of phagocytic processes (62) and host cell entry of several viruses such as Ebola virus (63), Middle East respiratory syndrome coronavirus [MERS-CoV, (64)] or SARS-CoV-II (65).

TPC-dependent Ca^{2+} liberation was shown to induce exocytosis, for instance, during release of cytolytic granules from T cells (66) or in interplay with TRPM4 during secretion of insulin (67). Consistently, the TRPM4 channel blocker 9-Phenantrol reduced internalization of *S. aureus* by host cells (**Figure 1**, B). Interestingly, exogenous addition of a bacterial SMase immediately before infection rescued the invasion defect in TPC1 and Syt7 K.O. cells (**Figure 2**, F) indicating that reduced invasion results from a decreased delivery of ASM to the host cell surface. Thus, NAADP-dependent Ca^{2+} liberation from lysosomal stores mediates Syt7-dependent fusion of lysosomes with the plasma membrane resulting in the release of ASM (**Figure 5**, F).

Inhibition of CD38, a known NAADP producer (49, 50), did not influence uptake of staphylococci (**Supp. Figure 1**, L). By contrast, we detected a decreased invasion in cells deficient for the Toll-like receptor adaptor protein SARM1, an alternative NAADP producer (52). However, the role of SARM1 in lysosomal exocytosis and ASM release requires further investigation. The impact of SARM1 on internalization of *S. aureus* was rather moderate, suggesting the existence of other NAADP-generating enzymes.

One important characteristic of the ASM-dependent internalization pathway is its velocity - taking place within the initial ten minutes of an infection with *S. aureus*, during which treatment with small molecules (**Figure 3**, D), as well as genetic ablation of TPC1 (**Figure 1**, E) and Syt7 (**Figure 2**, B) resulted in reduction of intracellular bacteria. This was accompanied by the quick formation of *S. aureus*-containing phagosomes decorated with fluorescent SM analogs (**Figure 3**, A; **Supp. Figure 3**, Supp. Video 1, Supp. Video 2).

When we blocked the rapid internalization pathway by ASM inhibitors (**Figure 4**, A, C; **Supp. Figure 4**, B), Vacuolin-1 (**Supp. Figure 4**, F) or by removal of surface SM (**Figure 4**, A, E; **Supp. Figure 4**, B, H), we observed changes in both, maturation of bacteria-containing vesicles and phagosomal escape. A delayed maturation of phagosomes may affect acidification of the vesicles, a property that is sensed by *S. aureus* leading to expression of a different subset of virulence factors (68) and hence may alter intracellular pathogenicity. Phagosomal escape of *S. aureus* only was dependent on SM on the plasma membrane during invasion but not on the presence of SM within the phago-endosome (**Figure 4**, D-G; **Supp. Figure 4**, H, I). This not only corroborated that phagosomal escape of clinically relevant *S. aureus* strains is independent of the bacterial SMase β-toxin (36), but also demonstrated that the outcome of phagosomal escape is influenced by processes at the plasma membrane during cell entry.

To exclude that inhibitor or bSMase treatments caused changes in phagosomal escape by affecting cellular processes other than bacterial uptake, we infected untreated WT cells with *S. aureus* for 10 or 30 min, respectively, and monitored phagosomal escape. Bacteria that invaded within the first 10 minutes after contacting host cells (“early invaders”) are predominantly ASM-dependent (**Figure 3**) and demonstrated significantly less phagosomal escape (**Figure 4**, G, H). Consistently, blocking the ASM-dependent pathway led to increased proportions of ASM-independent invaders, which in turn resulted in higher escape rates (**Figure 4**, C, E; **Supp. Figure 4**, F). Intracellular *S. aureus* infections thus are directly influenced by the mode of internalization. This ultimately resulted in lower host cytotoxicity (**Figure 5**, C-E; **Supp. Figure 6**) and bacterial replication (**Figure 5**, B) when we blocked the ASM-dependent invasion.

An uptake-related intracellular fate has been suggested for *Mycobacterium bovis* (39), *Toxoplasma gondii* (41) or *Brucella abortus* (42). However, in these studies the host cells were either depleted from cholesterol, which causes a variety of side effects (40), or internalization was artificially induced by chemicals or ectopic expression of receptors, respectively.

Taken together, we here describe a rapid internalization pathway for *S. aureus* into human epithelial and endothelial cells. Bacteria that enter the host cells via this infection route face a distinct intracellular fate. Here we show, to our knowledge, for the first time that host cells within the same population can be invaded by a pathogen via distinct routes and that this results in a differential infection outcome. Rapid internalization may prove beneficial for pathogens in an *in vivo* setting since internalization by host cells shortens the exposure to the innate immune system within a host. Interestingly, the absence of ASM in *Smpd1*$^{-/-}$ mice enhanced the potency of antibiotics to clear *S. aureus* sepsis (69). It is tempting to speculate that reduced host cell invasion in absence of ASM caused a prolonged exposure of the pathogen to antibiotics. Several FIASMAs are already approved drugs (70), and may have future use in infection treatment.

Acknowledgements

This work was supported by the Deutsche Forschungsgemeinschaft (DFG; *https://www.dfg.de*) within the research training group RTG2581 (M.R., F.S.). C.K. and C.A. are grateful to the DFG AR 376/22-1. M.R. was supported by funds of the Bavarian State Ministry of Science and the Arts and the University of Würzburg to the Graduate School of Life Sciences (GSLS), University of Würzburg. The DFG funded the Leica TCS SP5 CLSM under project code 116162193 and the BD FACSAriaIII cell sorter under project code 206080318.

We thank Sibylle Schneider-Schaulies and Thomas Rudel for valuable discussions and critically reading the manuscript, and Nadine Vollmuth as well as Christian Stigloher for scientific advice and intense discussions. We are indebted to Kathrin Stelzner for conducting FACS of cell lines and generation of *S. aureus* strains. pmRFP-LC3 was a gift from Tamotsu Yoshimori (Addgene plasmid # 21075; *http://n2t.net/addgene:21075*; RRID:Addgene_21075, (71)). pLVTHM (72), pMD2.G and psPAX2 (unpublished) were a gift from Didier Trono (Addgene plasmids # 12247, 12259 and 12260, respectively). pLX304-Flag-APEX2-NES was a gift from Alice Ting (Addgene plasmid # 92158, (73)) and pSpCas9(BB)-p2A-GFP (PX458) (74) was a gift from Feng Zhang (Addgene plasmid # 48138; *http://n2t.net/addgene:48138*). Figures were created in BioRender.

Additional information

Author Contributions

M.R., M.F. conceptualized the work, designed the methodology and wrote the original draft manuscript. M.F. acquired funding. M.R. F.S., K.U., M.P., A.M., N.K., J.W., A.I., C.K., K.P. performed the experiments; M.R., M.F. supervised the experiments. M.R., C.A., M.F. analyzed the data; all authors edited and revised the manuscript.

Declaration of interests

Patentability of PCK310 is currently evaluated by C.K. and C.A.

Materials and methods

Cell culture

HeLa (ATCC CCL-2^{TM}), 16HBE14o- (kindly provided by Prof. Jan-Peter Hildebrandt, University of Greifswald) and EA.hy 926 (75) were cultivated in RPMI+GlutaMAX^{TM} medium (Gibco^{TM}, Cat. No. 72400054) supplemented with 10% (v/v) heat-inactivated (56°C at 30 min) fetal bovine serum (FBS, Sigma Aldrich, Cat. No. F7524) and 1 mM sodium pyruvate (Gibco^{TM}, Cat.No. 11360088).

HuLEC-5a (ATCC CRL-3244^{TM}) and HuVEC (Gibco^{TM}, Cat. No.C01510C) were cultured in MCDB131 medium (Gibco^{TM}, Cat. No. 10372019) complemented with microvascular growth supplement (Gibco^{TM}, Cat. No. S00525), 2 mM GlutaMAX^{TM} (Gibco^{TM}, 35050061), 5 % (v/v) heat-inactivated (56°C at 30 min) FBS, 2.76 µM hydrocortisone (Sigma Aldrich, Cat. No. H0888), 0.01 ng/ml human epidermal growth factor (Pep Rotech, AF-100-15) and 1x Penicillin-Streptomycin (Gibco^{TM}, Cat. No. 15140122).

HeLa

HuLEC and HuVEC were detached by StemPro™ Accutase™ (Gibco™, Cat. No. A1110501) and seeded at the indicated density two days prior to the experiment, whereas HeLa, 16HBE14o-and EA.hy 926 were detached with TrypLE™ (Gibco™, Cat. No. 12604013) and seeded one day prior to the experiment.

Generation of HeLa KO cell lines

Generation of K.O. cell lines is based on a previous protocol (74). sgRNAs (**Table 1**) were designed with the CHOPCHOP online tool (chopchop.cbu.uib.no) and synthesized as primer pairs (Sigma Aldrich). After phosphorylation with T4 nucleotide kinase (ThermoFisher, Cat. No. ER0031), the sgRNAs were cloned into the BbsI sites of pSpCas9(BB)-p2A-GFP (AddGene #48138, (74)) via forced ligation by BbsI (ThermoFisher, Cat. No. ER1012) and T4 Nulceotide ligase (ThermoFisher, Cat. No. EL0011). The constructs were then transformed in *E. coli* DH5α (ThermoFisher, Cat. No EC0112) and subsequently sequence verified.

HeLa cells were transfected with 1 µg each of two distinct sgRNA constructs using JetPrime (Polyplus) following the manufacturer's instructions. After 36-48h, cells were sorted for strong GFP expression in a FACS Aria III (BD Bioscience). The resulting cell pools were cultivated and tested for loss of expression of the respective sgRNA target by Western Blotting.

Following antibodies were used: mouse anti-PTK7 monoclonal IgG1 (bio-techne, Cat. No. MAB4499) with a horse radish peroxidase (HRP)-conjugated anti-mouse antibody (SantaCruz, Cat. No. sc-516102) and rabbit anti-TPC1 polyclonal (Thermo Fisher, Cat. No. PA5-41048) with an HRP-conjugated anti-rabbit antibody (Biozol, Cat. No. 111-035-144).

Generation of reporter constructs

pLV-mRFP-CWT. mRFP and the cell wall-targeting domain of lysostaphin CWT were amplified using primers MP-mRFP-f and euk_mRFP-r, as well as infus-CWT-f and infus-CWT-r, respectively. As PCR templates we used pmRFP-LC3 (PMID 17534139) and pLV-YFP-CWT (76). The resulting plasmid was termed pLV-mRFP-CWT. The PCR products were subsequently cloned into pLVTHM (72) restricted with PmeI and SpeI by InFusion cloning following the manufacturer's recommendations.

pLV-YFP-Lysenin. The sequence of the sphingomyelin-binding but not pore-forming earthworm toxin mutant Lysenin^{W20A} (61) was synthesized by GeneArt (ThermoFisher) using a human codon usage and 5' flanking region encoding a glycine-rich linker sequence. The synthesized template served as template for subsequent PCRs.

Lysenin^{W20} was amplified using oligonucleotides InfReamp-f and hLysenin-infus-r (**Table 1**). YFP was amplified with Pm-eYFP-inf and eYFP-rev from template pLVTHM-YFP-CWT (76). Both PCR products were joined with pLVTHM vector restricted with PmeI and SpeI by InFusion cloning following the manuacturer's recommendations, thereby creating pLV-YFP-Lysenin.

Constructs were transformed into *E. coli* DH5α and sequences were validated. Plasmid preparations were performed using standard laboratory procedures. VSV-G-pseudotyped Lentiviral particles were generated by transfecting with each lentiviral vector as well as the plasmids pMD2.G (VSV G) and psPAX2 following the protocol of (72) and target cells were transduced as described previously (76).

Purpose	Name	sequence (5´→ 3´)
Gene deletion	Syt7-sgRNA2 rv	AAACATGACGTCATTGCGGCTGAG
	Syt7-sgRNA2 fw	CACCCTCAGCCGCAATGACGTCAT
	Syt7-sgRNA1 rv	AAACCACGATGAGTCCGACCGCCG
	Syt7-sgRNA1 fw	CACCCGGCGGTCGGACTCATCGTG
	TPCN1-sgRNA2 rv	AAACAGGACGGCGCTCCTCATCTT
	TPCN1-sgRNA2 fw	CACCAAGATGAGGAGCGCCGTCCT
	TPCN1-sgRNA1 rv	AAACTTCAGACCCCGTAAGTAATC
	TPCN1-sgRNA1 fw	CACCGATTACTTACGGGGTCTGAA
	SARM1-sgRNA1 rv	AAACTAGAGTCGAGCAACGGCACG
	SARM1-sgRNA1 fw	CACCCGTGCCGTTGCTCGACTCTA
	SARM1-sgRN2 rv	AAACGCACGTAGAATAGTTGGCGA
	SARM1-sgRNA2 fw	CACCTCGCCAACTATTCTACGTGC
Cloning	MP-mRFP-f	GAGACTAGCCTCGAGGTTTAAACCACCATGGCCTCCTCCGAGGACGTC
	euk_mRFP-r	GGAATGCCCGGGCGCGCCGGTGGAGTGGCGGC
	infus-CWT-f	ACCGGCGCGCCCGGGCATTCCACGCCCAATACAGGTTGG
	infus-CWT-r	GAGGTTGATTATCATATGACTAGTTCACTTTATAGTTCCCCAAAG
	eYFP-rev	CTTGTTGATGGGCTCGAGCCCTTGTACAGCTCGTCCATGCCGAG
	Pm-eYFP-inf	GACTAGCCTCGAGGTTTAAACCACCATGGTGAGCAAGGGCGAGGAG
	hLysenin-infus-r	GAGGTTGATTATCATATGACTAGTTCAGCCCACCACCTCCAG
	InfReamp-f	GGCTCGAGCCCATCAACAAG
	cYFP-f	ATGGTGAGCAAGGGCGAGGAGCTG
	his1-Flag-f	CATCATCATCATCACGGAGCGGACTACAAGGATGACGACGATAAGG
	his2-Inf-f	GACTAGCCTCGAGGTTTAAACCACCATGGCACATCATCATCATCATCA CGGAGCG
	Apex-YFP-infus-r	CGCCCTTGCTCACCATCTCGAGCCGTCCAGGGTCAGGCGCTCC

Table 1

Oligonucleotides used in this study

S. aureus culture

S. aureus liquid cultures were either grown in 37 g/L brain heart infusion (BHI) medium (Thermo Fisher, Cat. No. 237300) or in 30 g/l TSB medium (Sigma Aldrich, Cat. No. T8907). *E. coli* liquid cultures were grown in LB medium [10 g/l tryptone/peptone (Roth, Cat. No. 8952.4,) 5g/l yeast extract (Roth, Cat. No 2363.2), 10 g/l NaCl (Sigma Aldrich, Cat. No. S5886)].

For agar plates, 15 g/L agar (Otto Norwald, Cat. No. 257353), was added to either TSB (*S. aureus*) or LB (E. coli).

Media and plates were supplemented with appropriate antibiotics [5 µg/ml erythromycin (Sigma Aldrich, Cat. No. E5389), 10 µg/ml chloramphenicol (Roth, Cat. No. 3886.2), 100 ng/ml Carbenicillin (Roth, Cat. No. 6344.2)].

Strains used in this study are listed in **Table 2**.

S. aureus growth curves

S. aureus overnight cultures were grown in BHI medium, and 1 ml was centrifuged at 14,000 for 1 min. Bacteria were washed thrice with DPBS and either resuspended in BHI (for amitriptyline and ARC39 treatment) or infection medium [MCDB131 medium (Gibco^{TM}, Cat. No. 10372019) complemented with 2 mM GlutaMAX^{TM} (Gibco^{TM}, 35050061) and 10 % (v/v) heat-inactivated (56°C at 30 min) FBS, for ionomycin treatment). Bacteria suspensions were diluted to OD_{600}=0.1 in the respective medium. Then, 400 µL per well of the suspension as well as respective blanks were transferred into a 48 well plate and OD_{600} was determined every 16 min in Tecan mPlex200 microplate reader.

S. aureus infections

Host cells were seeded in 6 well plates ($2x10^5$ cells per well), 12 well plates ($1x10^5$ cells per well) or 24 well plates ($0.5x10^5$ cell per well) either one day (HeLa, EA.hy 926, 16HBE14o$^-$) or two days (HuLEC, HuVEC) prior to the experiment. Host cells were washed thrice with DPBS and infection medium or Ca^{2+}-free infection medium [DMEM w/o calcium (Gibco^{TM}, Cat. No. 21068028) complemented with 10 % (v/v) heat-inactivated (56°C at 30 min) FBS and 200 µM BAPTA (Merck Millipore, 196418)] with or without 1.8 mM $CaCl_2$ (Roth, Cat. No. 5239.1) was added. If indicated, cells were pretreated with compounds prior to infection (for details about treatments see **Table 1**). For experiments involving blocking of receptors by antibodies, respective solvent controls were implemented (final concentrations in infection medium: 0.002% (w/v) NaN_3 (Sigma Aldrich, Cat. No. S2002) 5% glycerol (Roth, Cat. No 3783.2) in 10% DPBS for 30 ng/ml anti-NRCAM antibody as well as well as 0.01 % (w/v) NaN_3 for 50 ng/ml anti-CD73 and 50 ng/ml anti-MELTF antibodies.

An *S. aureus* overnight culture grown in BHI containing the appropriate antibiotics was diluted to an OD_{600}=0.4 in the same medium. When inducible expression of genes was required for the strains *S. aureus* JE2 p*Cer* and *S. aureus* JE2 p*Cer+hlb,* 200 ng/ml anhydrous tetracycline (AHT, AcrosOrganics, 233131000) was added. The culture was grown to an OD_{600}= 0.6-1.0 and 1 ml bacterial suspension was harvested by centrifugation and washed twice with Dulbecco's Phosphate Buffered Saline (DPBS, Gibco^{TM}, Cat. No 14190169). The bacteria were resuspended in infection medium (or Ca^{2+}-free infection medium when infection was performed in absence of extracellular Ca^{2+}). The number of bacteria per ml in the suspension was determined with a Thoma counting chamber and the MOI was determined. If not indicated otherwise, an MOI=10 was used for infections.

Strain	Remarks	Source
S. aureus 6850		(77)
S. aureus 6850 Δ*hlb*	deficient in β-toxin production	(36)
S. aureus Cowan I	NCTC 8530, isolated from septic arthritis, agr dysfunction, low expression of toxins and proteases	ATCC 12598
S. aureus JE2	MRSA, USA300	(78)
S. aureus JE2 Δ*hla*	deficient in α-toxin production	(79)
S. aureus JE2 Δ*hlb*	deficient in β-toxin production	(45)
S. aureus JE2 SarAP1 Cerulean	Constitutive expression of the fluorescence protein Cerulean	This work
S. aureus JE2 SarAP1 mRFP	Constitutive expression of the fluorescence protein mRFP	(38)
S. aureus JE2 p*Cer*	Anhydrous tetracycline (AHT) inducible expression of Cerulean, construct published in (80) and was transduced into *S. aureus* JE2	This work
S. aureus JE2 p*Cer+hlb*	Anhydrous tetracycline (AHT) inducible expression of Cerulean and β-toxin, construct published in (80) and was transduced into *S. aureus* JE2	This work
S. aureus Cowan I *SarAP1 Cerulean*	Constitutive expression of the fluorescence protein Cerulean	This work
S. aureus 6850 SarAP1 Cerulean	Constitutive expression of the fluorescence protein Cerulean	(38)
S. aureus 6850 Δ*hlb* SarAP1 Cerulean	Constitutive expression of the fluorescence protein Cerulean	This work

Table 2

Bacterial Strains used in this study

compound	Supplier/Cat.No.	preincubation time	removal prior to infection?
2-APB (2-Aminoethoxydiphenylborate)	Sigma Aldrich/ D9754	75 min	removed prior to infection
8-Bromo-cADPR (8-Bromo-cyclic ADP ribose)	Biolog/065-005	75 min	present during infection
9-Phenantrol	Biomol/ Cay15248-50	75 min	present during infection
amitriptyline	Sigma Aldrich/ A8404	75 min	present during infection
ARC39	(57)	18 h, add fresh inhibitor for another 4h or as indicated	present during infection
BAPTA-AM	Merck Millipore/ 196419; (44)	25 min	removed prior to infection
BODIPY-FL™-C12-Ceramide	Santa Cruz/ sc-503923	90 min	present during infection
BODIPY-FL™-C12-Sphingomyelin	ThermoFisher/D7711	90 min	present during infection
CD38i/78c	Sigma Aldrich/ 5387630001	75 min	present during infection
Ionomycin	Sigma Aldrich/ I0634	75 min	present during infection
PCK310	To be published elsewhere	4h or as indicated	present during infection
trans-Ned19	Sigma Aldrich/ SML2830; (48)	75 min	present during infection
Vacuolin-1	Biozol/ MCE-HY-118630	75 min	present during infection
β-toxin	Sigma Aldrich/ S8633	75 min	removed prior to infection if not indicated otherwise

Table 3

Host cell treatment with various compounds

The infection was synchronized by centrifugation 800xg/8 min/RT (end of the centrifugation: t=0). To determine bacterial invasion, the infection was stopped after 30 min (unless indicated otherwise) by removing extracellular bacteria with 20 µg/ml Lysostaphin (AMBI, Cat. No. AMBICINL) in infection medium for 30 min. Then, host cells were washed thrice with DPBS, lysed by addition of 1 ml/well (12 well plate) or 0.5 ml/well (24 well plate) Millipore water and the number of bacteria in lysates was determined by plating serial dilutions (10^{-1}, 10^{-2}, 10^{-3}) on TSB agar plates. Plates were incubated overnight at 37 °C and CFU were enumerated. To determine invasion efficiency, the number of bacteria determined in tested samples were normalized to untreated controls (set to 100%).

For measuring invasion dynamics, the number of bacteria was either normalized to the 30 min time point of untreated controls or to the corresponding time points of untreated controls.

If later time points in infection were investigated, infection medium containing 2 µg/ml Lysostaphin was added to the cells until the indicated time.

For testing bacterial susceptibility to inhibitors (“survival”) or adherence, Lysostaphin treatment was omitted, and host cells were immediately lysed by addition of Millipore water or washed five times with DPBS and subsequently lysed with Millipore water, respectively. The number of bacteria in lysates was determined by CFU counting (dilutions 10^{-2}, 10^{-3}, 10^{-4}) on TSB agar plates.

Phagosomal escape assays

For phagosomal escape assays with amitriptyline, ARC39, PCK310 and β-toxin, HeLa cells expressing RFP-CWT and Lysenin^{W20A}-YFP were infected with the indicated *S. aureus* strain as described in the previous paragraph. Infections with *S. aureus* JE2 p*Cer* and *S. aureus* JE2 p*Cer+hlb* were carried out in presence of 200 ng/ml AHT.

For phagosomal escape assays, HeLa cells expressing RFP-CWT and Lysenin^{W20A}-YFP were infected for 10 min (early invaders) or 30 min (early and late invaders) at the indicated MOIs.

For the phagosomal escape assays with two *S. aureus* JE2 strains expressing different fluorescence proteins, HeLa cells expressing YFP-CWT were infected with an MOI=5 of an initial *S. aureus* JE2 strain (*S. aureus* JE2 SarAP1 Cerulean or *S. aureus* JE2 SarAP1 mRFP). After 12 min of infection, a second infection pulse was initiated by adding the second *S. aureus* JE2 strain (expressing the complementary fluorescence protein, *S. aureus* JE2 SarAP1 mRFP or *S. aureus* JE2 SarAP1 Cerulean, respectively) and centrifuging the bacteria on the host cells. To exclude that the type of fluorescence protein expressed by the *S. aureus* strains contributes to the experimental outcome, either strain was used for the first and second infection pulse (each combination: n=4).

Phagosomal maturation assays

To monitor phagosomal maturation, HeLa cells expressing mCherry-Rab5 and YFP-Rab7 or YFP-Rab7 and RFP-CWT were infected with *S. aureus* JE2 SarAP1 Cerulean.

After 3 h p.i. (unless indicated otherwise), cells were washed thrice with DPBS and fixed with 0.2% glutaraldehyde (Sigma Aldrich, Cat. No. 10333) / 4% paraformaldehyde in PBS (Morphisto, Cat. No 11762.01000) for 30 min at RT. Then, cells were washed thrice with DPBS, stained with 5µg/ml Hoechst 34580 (Thermo Fisher, Cat. No. H21486) and mounted in Mowiol [24g glycerol (Roth, Cat. No. 3783.2), 9.6 g Mowiol®4-88 (Roth, Cat. No 0713.2), 48 ml 0.2 M TRIS-HCl pH 8.5 (Sigma Aldrich, Cat. No T1503), 24 ml Millipore water].

Samples were imaged with a Leica TCS SP5 confocal microscope (Wetzlar, Germany; Software Leica LAS AF Version 2.7.3.9723) with a 40x immersion oil objective (NA1.3) and a resolution of 1024x1024 pixels [Cerulean (Ex. 458 nm/Em. 460-520), YFP (Ex. 514 nm/Em. 520-570nm),

mRFP/mCherry (Ex. 561 nm/Em.571-635nm) and Hoechst 34580 (Ex. 405 nm/Em.410-460nm). At least 10 fields of view per samples were recorded.

Image analysis was performed in Fiji (81) using a previously described macro (80) that identifies and extracts individual bacteria from images as regions of interest (ROIs, see **Supp. Figure 5**). Subsequently, fluorescent intensity in every channel is measured to determine recruitment of fluorescence reporters to the bacteria. Results were exported as text files and proportion of bacteria that recruited individual reporters was determined with the Flowing 2 software (Turku Bioscience Center). Phagosomal escape rates were determined as the proportion of CWT-positive bacteria of the total number of intracellular bacteria. Similarly, the proportion of Lysenin^{W20A}-positive escape events, the ratio of Lysenin^{W20A}-/CWT-positive events and all CWT-positive events was calculated.

To measure the proportion of bacteria that were associated with Rab5 and/or Rab7, the proportion of Rab5- and/or Rab7-positive membranes around bacteria of all intracellular bacteria was determined. For experiments obtained with HeLa cells expressing YFP-Rab7 and RFP-CWT, bacteria that acquired RFP-CWT were removed from the dataset. Subsequently, the proportion of Rab7-positive bacteria in relation to all CWT-negative intracellular bacteria was determined.

Live cell imaging

The indicated host cells were seeded one (HeLa) or two days (HuLEC) prior to the experiments in µ-slide 8 well live cell chambers (ibidi, Cat. No 80826-90) with a density of 0.375x10^5 cells per well. For monitoring host cell entry, cells were washed thrice with DPBS and were then, incubated for 90 min in infection medium with 1 µM BODIPY-FL-C$_{12}$-sphingomyelin (Thermo Fisher Cat. No. D7711), 10 µM BODIPY-FL-C$_{12}$-ceramide (Santa Cruz, Cat.No. sc-503923) or 10 µM visible-range FRET probe (59). Pretreatment with the FRET probe was performed in infection medium containing 1 % (v/v) FBS. Then, cells were washed thrice with DPBS and imaging medium [RPMI 1640 w/o phenol red (Gibco^{TM}, Cat. No. 11835030) containing 10% (v/v) heat-inactivated (56°C/30 min) FBS (Sigma Aldrich, Cat. No. F7524) and 30 mM HEPES (Gibco^{TM}, Cat.No. 15630080)] applied. Samples stained with the FRET probe were imaged in imaging medium containing 1% FBS and in presence of 10 µM FRET probe. Samples were infected with *S. aureus* JE2 SarAP1 Cerulean (FRET probe samples) or *S. aureus* JE2 SarAP1 mRFP (BODIPY-FL-C12-sphingomylein/-ceramide) at an MOI=50 without synchronization by centrifugation. Infection was monitored with a Leica TCS SP5 confocal microscope (Wetzlar, Germany) in intervals of 1 min by recording BODIPY-FL (Ex. 496 nm/Em. 500-535 nm), mRFP (Ex. 561 nm/Em.571) FITC (Ex. 488 nm/Em. 500-560), Cerulean (Ex. 458 nm/Em. 460-520), BODIPY-TR (Ex. 594 nm/Em. 610-680) and FRET (Ex.488 nm/ Em:610-680) channels. Cells were recorded with a 40x immersion oil objective and a resolution of 2048x2048 pixels. For samples stained with the FRET probe, 20 µg/ml lysostaphin was added 40 min p.i. to remove extracellular bacteria. For quantification of bacteria that associate with BODIPY-FL-C$_{12}$-sphingomyelin/-ceramide, individual bacteria in single frames were identified, extracted as ROIs and BODIPY-FL fluorescence in ROIs was measured in Fiji (81) as described before for phagosomal escape assays. Results were extracted as text files and the proportion of bacteria associating with BODIPY-FL was determined with Flowing2 (Turku Bioscience Center).

For monitoring intracellular *S. aureus* infection, host cells were pretreated and infected with *S. aureus* JE2 SarAP1 Cerulean (HeLa RFP-CWT/Lysenin^{W20A}-YFP) or *S. aureus* JE2 SarAP1 mRFP (HuLEC) as described in "*S. aureus* infection". HuLEC additionally were treated with 1 µM BODIPY-FL-C$_{12}$-sphingomyelin in infection medium for 90 min and washed thrice with DPBS before the indicated treatment was applied. After extracellular bacteria were removed with 20 µg/ml lysostaphin for 30 min, imaging medium containing 2 µg/ml lysostaphin was applied and infections were monitored in intervals of 5 min (HeLa RFP-CWT) or 20 min (HuLEC). Phagosomal escape was evaluated in Fiji as described above. To determine intracellular replication, the

number of bacteria was determined for each individual frame as described before (80). The number of bacteria at each time point was then normalized to the number of bacteria detected in the first frame to calculate the relative replication.

ASM and NSM activity assays

Thin layer chromatography (TLC)-based ASM/NSM activity assays were adapted from previously published protocols (58). To determine cellular ASM activity, the indicated cell lines were seeded in 24 well plates with a density of $1x10^5$ cell per well one day (HeLa, EA.hy 926, 16HBE14o$^-$) or two days (HuLEC, HuVEC) prior to the experiment. Cells were either treated with 20 µM amitriptyline or with 10 µM ARC39 for 22 h (fresh inhibitor was applied after 18h) in infection medium. Then, cells were washed thrice and lysed by addition of 100 µL per well ASM lysis buffer [250 mM NaOAc pH 5 (Roth, Cat. No 6773.2), 0.1% Nonidet® P40 substitute (AppliChem. Cat. No. A1694,0250), 1.3 mM EDTA 1.3 mM (Roth, Cat. No. 8040.2), 1x protease inhibitor cocktail (Sigma Aldrich, 11873580001)] for 15 min/4°C. Cells were scraped from the substratum and protein concentration in the resulting lysates was measured with a Pierce™ bicinchoninic acid (BCA) assay kit (Thermo Fisher, Cat. No. 23227). 1 µg of protein was incubated with 100 µL ASM lysate assay buffer [200 mM NaOAc pH 5 (Roth, Cat. No 6773.2), 0.02 % Nonidet® P40 substitute (AppliChem. Cat. No. A1694,0250), 500 mM NaCl (VWR, Cat. No. 27810.364)] containing 0.58 µM BODIPY-FL-C_{12}-Sphingomyelin (Thermo Fisher, Cat. No. D7711) for 4h at 37°C and 300 rpm.

For measuring bacterial SMase/NSM activity in *S. aureus* cultures, an overnight culture of the indicated strain was grown in BHI medium, centrifuged 14.000xg and the supernatant was sterile filtered with 0.2 µm filter. 100 µL of sterile supernatant was incubated with 100 µL NSM assay buffer [200 mM HEPES, pH 7.0 (Roth, Cat. No. 6763.3), 200 mM $MgCl_2$ (Roth, Cat.No. 2189.2), 0.05% Nonidet P-40 (AppliChem. Cat. No. A1694,0250)] for 4h/37°C/300 rpm.

The reactions were stopped by addition of 2:1 $CHCl_3$:MeOH (Roth, Cat. No. 3313.2 and Cat. No. 8388.6). Samples were vortexed, centrifuged at 13,000 x g for 3 min and 50-100 µL of the lower organic phase were transferred to a fresh tube. Samples were completely evaporated using a SpeedVac 5301 concentrator (Eppendorf), resuspended in 10 µL 2:1 $CHCl_3$/MeOH and spotted in 2.5 µL aliquots on a TLC plate (Alugram, Xtra Sil G/UV254, 0.2 mm/silica gel 60; VWR, Cat. No. 552-1006).

Plates were developed using 80:20 $CHCl_3$ and subsequently scanned with a Typhoon 9200 Scanner (Amersham). For quantification, intensities of the lower (SM) and the upper bands (Cer) were measured in Fiji (81) and activity was determined based on the reaction time, protein amount and SM/Cer ratios. For the flow cytometry based read out, cells seeded in a density of $0.5x10^5$ cells per well in a 24 well plate either one day (HeLa, EA.hy 926, 16HBE14o$^-$) or two days (HuLEC, HuVEC) prior to the experiment. Cells were treated with ARC39 and amitriptyline as described above. Then, cells were washed thrice with DPBS and incubated with 10 µM FRET probe (59) for 2h in presence of the inhibitors. Subsequently, cells were washed thrice, detached with TrypLE™ (Gibco™, Cat. No. 12604013) and resuspended with 2% (v/v) FBS in DPBS. Samples were analyzed for FITC (Ex. 488 nm/Em. band pass 530/30 nm) and BODIPY-TR (Ex.: 561nm/ Em. band pass 695/40nm) fluorescence with Attune NxT flow cytometer (Thermo Fisher, Attune Cytometric Software v5.2.0). Cell populations were analyzed for FITC and BODIPY-TR mean fluorescence in Flowing 2 (Turku Bioscience Center) and FITC vs. BODIPY-TR ratios were calculated to determine arbitrary probe conversion.

Cytotoxicity Assays

For all cytotoxicity assays, HuLEC were seeded in 24 well plates with a density of $0.5x10^5$ cells per well two days prior to the experiment. Then, cells were infected with *S. aureus* JE2 with the indicated MOI as described in "*S. aureus* infection" and cytotoxicity was determined 21 h p.i. For

cytotoxicity measurements upon ionomycin treatment, cells were incubated with the indicated concentration of ionomycin in infection medium for 75 min and then, cytotoxicity assays were conducted.

Lactate dehydrogenase (LDH) assay was performed with the Cytotoxicity Detection KitPLUS (LDH, Sigma Aldrich, Cat. No. 4744934001) according to manufacturer's instructions.

For annexin V and 7-Aminoactinomycin D (7-AAD) assays, cells were washed thrice with DPBS, detached with 250 µL per well trypsin and resuspended in 250 µL per well staining buffer [1.7% (v/v) APC Annexin V (BD Pharmingen^{TM}, Cat. No. 550475), 1.7% (v/v) 7-AAD (BD Pharmingen^{TM}, Cat No. 559925), 2% (v/v) heat-inactivated (56°C/30 min) FBS (Sigma Aldrich, Cat. No. F7524), 4 mM $CaCl_2$ (Roth, Cat. No. 5239.1) in DPBS]. After incubation for 10 min/RT, cells were analyzed with a Attune NxT flow cytometer for 7-AAD (Ex. 488 nm/Em. band pass 695/40 nm) and APC (Ex. 637 nm/Em. band pass 670/14 nm). Cell populations were analyzed with Flowing2 (Turku Biosciences Center) and gates were adjusted according to untreated control cells. To determine the proportion of cells that remained attached to the substratum during the infection, number of cells was determined based on the number of detected single cells, flow rate and sample volume.

Statistical analysis

Statistical analysis was performed in GraphPad prism (V10.1.2). One-sample t-test was used for analysis of normalized data sets. Otherwise, one- or two-way ANOVA, dependent on the number of variables, was used in combination with suitable multiple comparisons testing. Details about sample size and deployed statistical analysis can be found in respective figure legends. All data are shown as mean ± standard deviation.

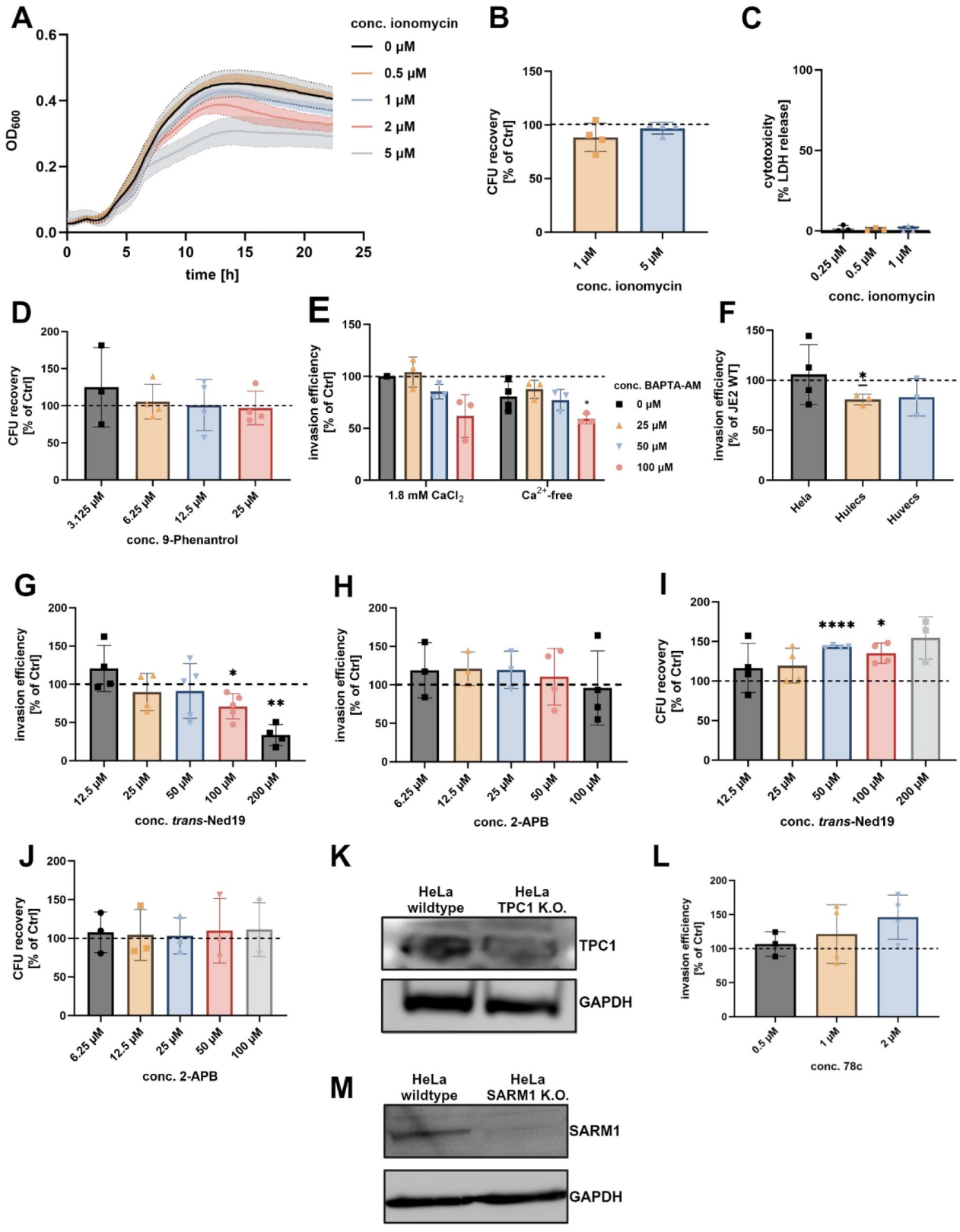
A
conc. ionomycin
0 µM
0.5 µM
1 µM
2 µM
5 µM
OD600
time [h]
B
CFU recovery [% of Ctrl]
conc. ionomycin
C
cytotoxicity [% LDH release]
conc. ionomycin
D
CFU recovery [% of Ctrl]
conc. 9-Phenantrol
E
invasion efficiency [% of Ctrl]
conc. BAPTA-AM
0 µM
25 µM
50 µM
100 µM
1.8 mM CaCl2
Ca2+-free
F
invasion efficiency [% of JE2 WT]
Hela
Hulecs
Huvecs
G
invasion efficiency [% of Ctrl]
conc. trans-Ned19
H
invasion efficiency [% of Ctrl]
conc. 2-APB
I
CFU recovery [% of Ctrl]
conc. trans-Ned19
J
CFU recovery [% of Ctrl]
conc. 2-APB
K
HeLa wildtype
HeLa TPC1 K.O.
TPC1
GAPDH
L
invasion efficiency [% of Ctrl]
conc. 78c
M
HeLa wildtype
HeLa SARM1 K.O.
SARM1
GAPDH

Supp. Figure 1

Supporting information for Ca^{2+}-dependent internalization of *S. aureus*.

(A) High ionomycin concentrations interfere with growth of *S. aureus* JE2. *S. aureus* JE2 was grown in in presence of varying concentrations of ionomycin. Growth (OD_{600}) was determined in a microplate reader. (B) **Ionomycin does not affect survival of *S. aureus* JE2 during infection of host cells.** HeLa cells were pretreated with varying concentrations of ionomycin and subsequently, infected with *S. aureus* JE2. After 30 min, cells were lysed and surviving extra- and intracellular bacteria were recovered by CFU count. **(C) Ionomycin does not affect host cell survival.** HeLa cells were treated with the indicated concentrations of ionomycin, and cytotoxicity was determined by measuring in lactate dehydrogenase (LDH) release. (**D) 9-Phenantrol does not affect survival of *S. aureus* JE2.** HeLa cells were pretreated with varying concentrations of 9-Phenantrol and infected with *S. aureus* JE2. After 30 min, cells were lysed and surviving extra- and intracellular bacteria were recovered by CFU plating. (**E) Chelation of intracellular but not presence of extracellular Ca^{2+} affects *S. aureus* internalization by HeLa cells.** HeLa cells were preloaded with varying concentrations of the cell-permeable Ca^{2+} chelator BAPTA-AM and then infected with *S. aureus* JE2 in presence (+1.8 mM $CaCl_2$) or absence (Ca^{2+}-free) of Ca^{2+} in the cell culture medium. Invasion efficiency was determined by CFU plating. (**F) α-toxin plays only a subordinate role during *S. aureus* uptake by host cells.** HeLa, HuLEC or HuVEC were infected with *S. aureus* JE2 wildtype or a strain deficient in α-toxin production (Δ*hla*). Invasion efficiency was determined by CFU plating. The number of intracellular bacteria was normalized to samples infected with the wildtype. **(G, H) *trans*-Ned19 but not 2-APB affects invasion of *S. aureus* JE2 in HeLa.** HeLa cells were pre-treated with *trans*-Ned19 (**G**) or 2-APB (**H**). 2-APB was removed from the cells shortly before infection to avoid direct contact of inhibitor and bacteria (due to a bactericidal effect of 2-APB; data not shown). Then, cells were infected with *S. aureus* JE2 and invasion efficiency was determined. **(I, J) *trans*-Ned19 and 2-APB have no effect on *S. aureus* JE2 in our infection protocol.** HeLa cells were pre-treated with or 2-APB (**I**) or *trans*-Ned19 (**J**). 2-APB was removed from the cells shortly before infection. Then, cells were infected with *S. aureus* JE2 and, after 30 min, total bacteria (extra- and intracellular) were recovered by CFU plating. (**K) Reduction of TPC1 expression in a Cas9-treated cell pool (HeLa TPC1 K.O.).** TPC1 as well as GAPDH (loading control) was detected in lysates of wildtype and TPC1 K.O. cells via Western blot. **(L) CD38 is not enrolled in *S. aureus* internalization.** HeLa cells were pretreated with the CD38 inhibitor 78c and invasion efficiency of *S. aureus* JE2 was determined. (**M) Reduction of SARM1 expression in a Cas9-treated cell pool (HeLa SARM1 K.O.).** TPC1 as well as GAPDH (loading control) was detected in lysates of wildtype and SARM1 K.O. cells via Western blot. Statistics: one sample t-test, Bars represent mean +/- SD. *p≤0.05, **p≤0.01, ***p≤0.001, ****p≤0.0001.

Created with *BioRender.com/h92e766*.

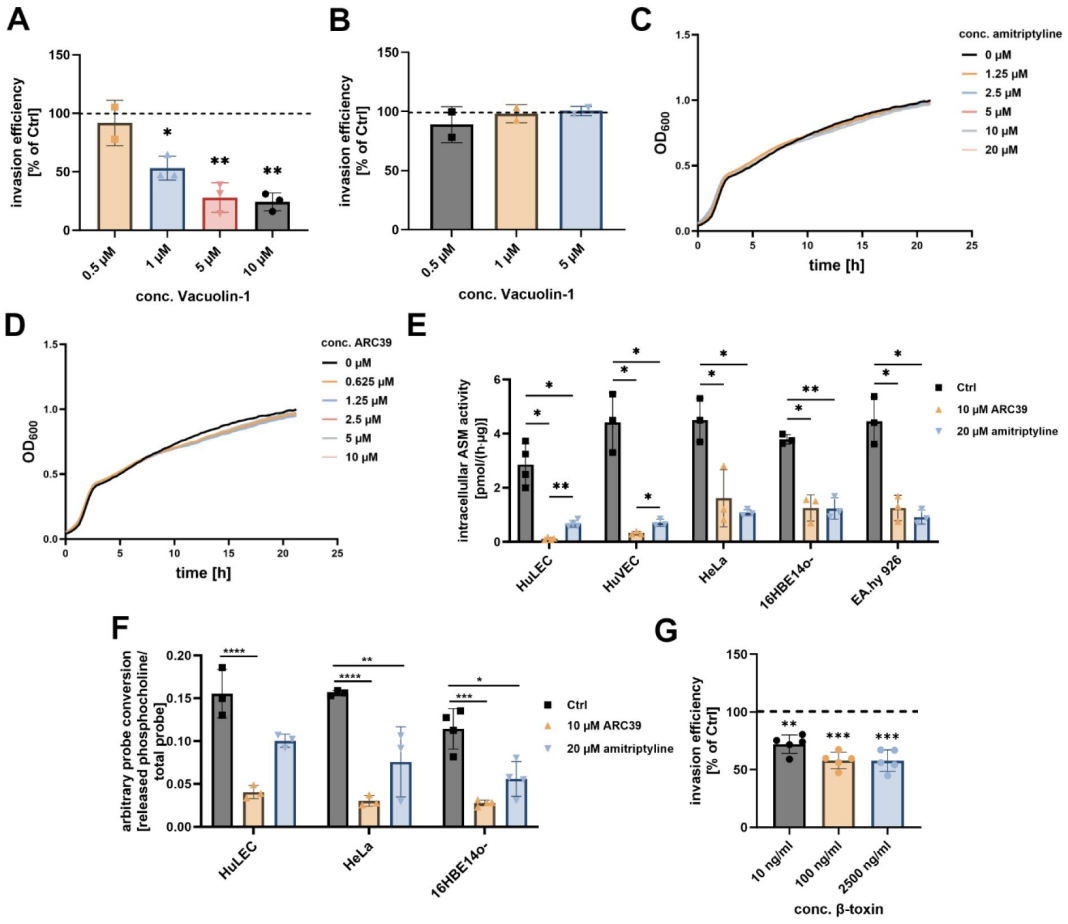

Supp. Figure 2

Supporting information for the involvement of lysosomal exocytosis and ASM in *S. aureus* invasion

(A) Blocking lysosomal exocytosis by Vacuolin-1 reduces *S. aureus* invasion in HeLa. HeLa cells were treated with increasing concentrations of the lysosomal exocytosis inhibitor Vacuolin-1. The invasion efficiency of *S. aureus* JE2 was determined 30 min p.i. **(B) Vacuolin-1 has no bactericidal effect.** HeLa cells were treated with Vacuolin-1 and infected with *S. aureus* JE2. After 30 min, total bacteria (extra- and intracellular) were recovered by CFU plating and normalized to untreated controls. **(C, D) The ASM inhibitors amitriptyline and ARC39 have no effect on growth of *S. aureus*.** *S. aureus* JE2 was grown in presence of varying concentrations of amitriptyline (**C**) or ARC39 (**D**) in BHI medium and growth was determined by measuring OD_{600} in a microplate reader. **(E, F) ASM activity and ASM inhibition by ARC39 and amitriptyline is similar among human cell lines.** Several cell lines were treated with amitriptyline or ARC39 and ASM activity within cell lysates was assessed by either thin layer chromatography-based TLC-based ASM activity assays, the conversion of BODIPY-C12-SM (**E**), or by a flow cytometry-based ASM activity assay and conversion of visible-range FRET probe (**F**). **(G) Removal of SM from the plasma membrane by β-toxin affects *S. aureus* host cell.** HeLa cells were pretreated with the indicated concentrations of β-toxin and subsequently the invasion efficiency of *S. aureus* JE2 was determined. Statistics: one sample t-test (A, G), mixed-effects model (REML) and Tukey's multiple comparison (E, F), Bars represent mean +/- SD. *p≤0.05, **p≤0.01, ***p≤0.001, ****p≤0.0001.

Created with *BioRender.com/d19d047*.

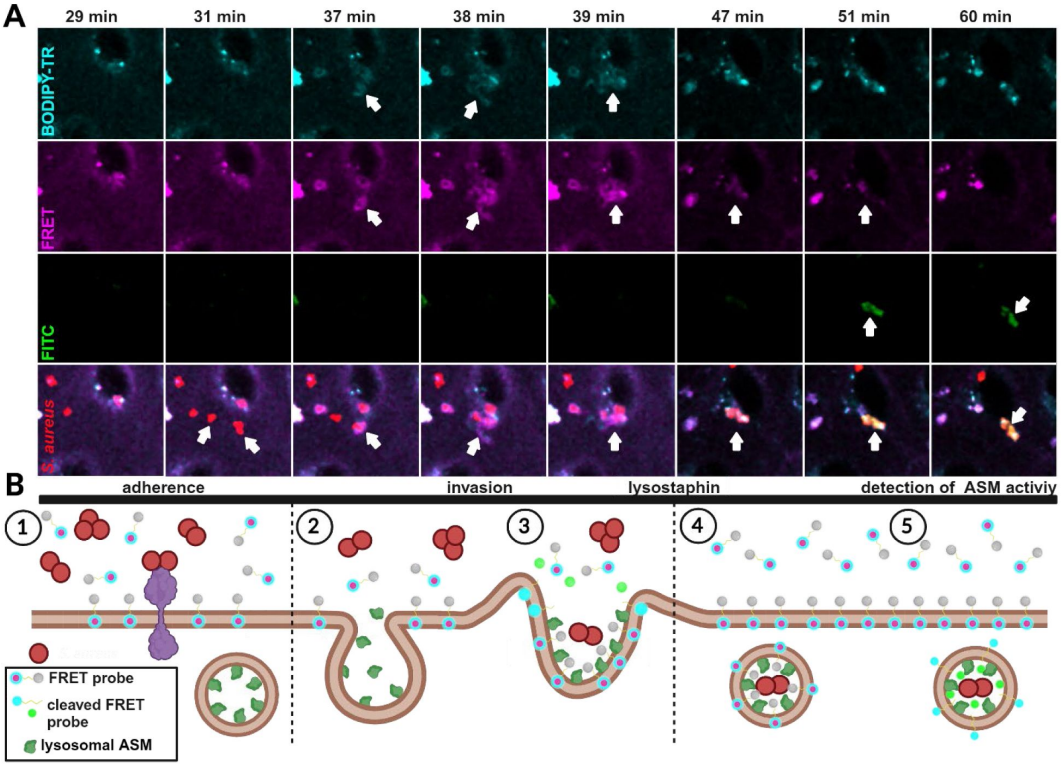

Supp. Figure 3

S. aureus associates with a visible-range SM probe during host cell invasion.

(A) Live cell imaging of *S. aureus* infection reveals association of the bacteria with a SM analog during cell entry. HuLEC were treated with 10 µM of a visible range FRET probe in presence of 1% FBS. Then, cells were infected with *S. aureus* JE2 in presence of the probe and infection was monitored by live cell confocal imaging. After 40 min, lysostaphin was added to remove extracellular bacteria. The BODIPY-TR signal demonstrates the localization of the probe, the FRET signal indicates an intact, non-metabolized probe, whereas FITC fluorescence indicates probe cleavage by ASM. Bacteria of interest (white arrows) adhere to host cell between 29 and 31 min p.i. **(B) Hypothetical model of *S. aureus* invasion.** (1). The interaction of bacteria with the host cell surface triggers lysosomal exocytosis, release of ASM (2) and the uptake of the bacteria (cmp. to A: at 37-39 min p.i.) by ASM-dependent membrane remodeling (3). ASM is co-internalized together with bacteria (4) and subsequently, cleaves the probe within the *S. aureus*-containing phagosome (5) (cmp: to A: increasing FITC signal starting at 47 min p.i.).
Created with *BioRender.com/g00y645*.

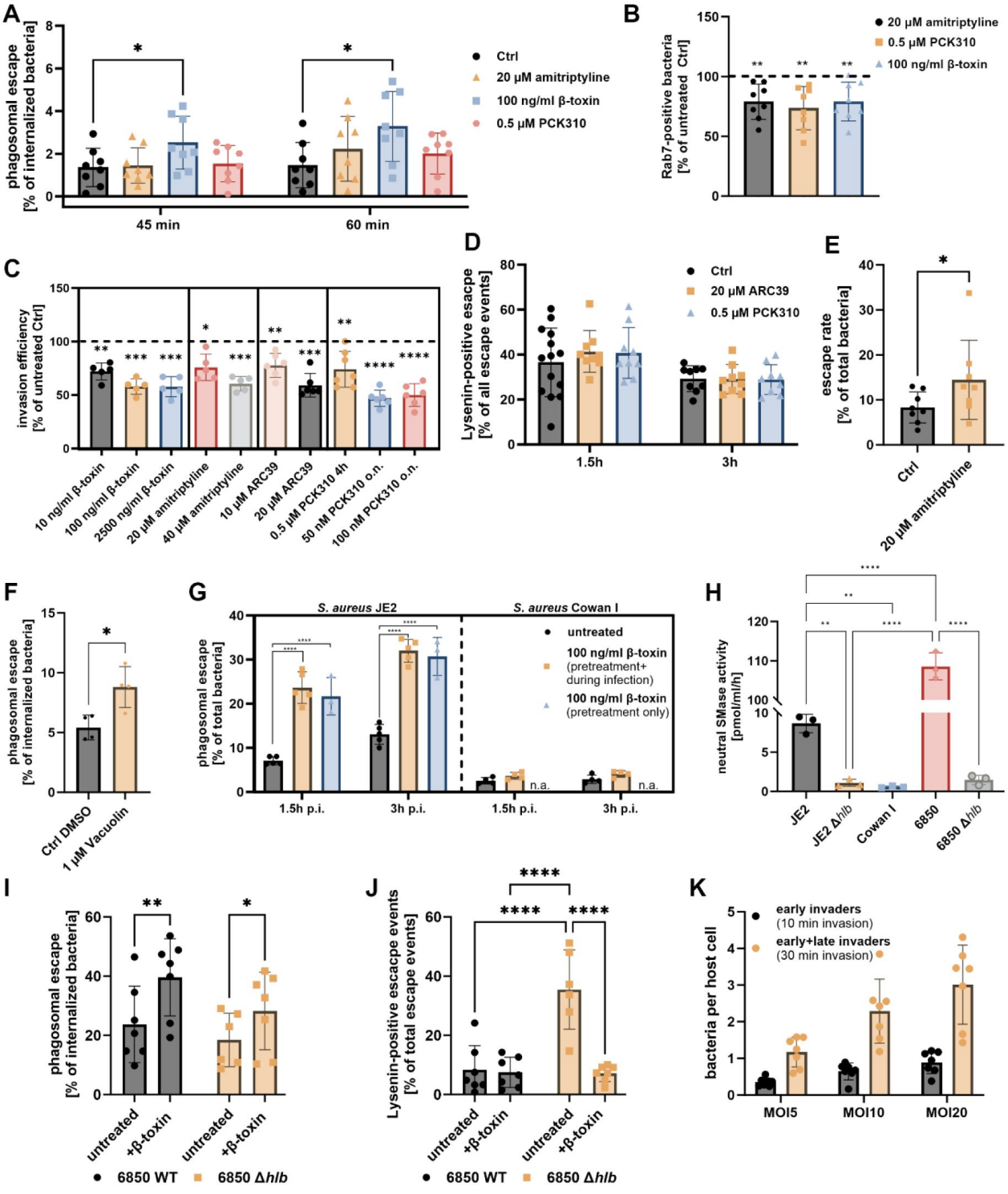
A
phagosomal escape [% of internalized bacteria]
45 min
60 min
Ctrl
20 µM amitriptyline
100 ng/ml β-toxin
0.5 µM PCK310
B
Rab7-positive bacteria [% of untreated Ctrl]
20 µM amitriptyline
0.5 µM PCK310
100 ng/ml β-toxin
C
invasion efficiency [% of untreated Ctrl]
10 ng/ml β-toxin
100 ng/ml β-toxin
2500 ng/ml β-toxin
20 µM amitriptyline
40 µM amitriptyline
10 µM ARC39
20 µM ARC39
0.5 µM PCK310 4h
50 nM PCK310 o.n.
100 nM PCK310 o.n.
D
Lysenin-positive esacpe [% of all escape events]
Ctrl
20 µM ARC39
0.5 µM PCK310
1.5h
3h
E
escape rate [% of total bacteria]
Ctrl
20 µM amitriptyline
F
phagosomal escape [% of internalized bacteria]
Ctrl DMSO
1 µM Vacuolin
G
S. aureus JE2
S. aureus Cowan I
phagosomal escape [% of total bacteria]
untreated
100 ng/ml β-toxin (pretreatment+ during infection)
100 ng/ml β-toxin (pretreatment only)
n.a.
1.5h p.i.
3h p.i.
H
neutral SMase activity [pmol/ml/h]
JE2
JE2 Δhlb
Cowan I
6850
6850 Δhlb
I
phagosomal escape [% of internalized bacteria]
untreated
+β-toxin
6850 WT
6850 Δhlb
J
Lysenin-positive escape events [% of total escape events]
untreated
+β-toxin
6850 WT
6850 Δhlb
K
bacteria per host cell
early invaders (10 min invasion)
early+late invaders (30 min invasion)
MOI5
MOI10
MOI20

Supp. Figure 4

Supporting information for phagosomal maturation and phagosomal escape measurements.

(A) Phagosomal escape assay in early infection. A HeLa reporter cell line expressing YFP-Rab7 and RFP-CWT was treated with amitriptyline, β-toxin and PCK310 and subsequently infected with *S. aureus* JE2 for 30 min. Extracellular bacteria were removed by lysostaphin and the proportion of bacteria that acquired the phagosomal escape marker RFP-CWT was determined 45 and 60 min p.i. (n=8). **(B) Reduced association of *S. aureus* with Rab7 is not due to changes in phagosomal escape.** HeLa cells expressing YFP-Rab7 and the phagosomal escape marker RFP-CWT were treated with amitriptyline, PCK310 or β-toxin and subsequently, infected with *S. aureus* JE2 for 45 min and analyzed by CLSMs. Bacteria that escaped from phagosomes were subtracted from the data set and the proportion of residual bacteria associating with Rab7 was determined. Results of treated samples were normalized to untreated controls (n=7). **(C) β-toxin treatment and ASM inhibition reduced invasion efficiency of *S. aureus* JE2 in a dual reporter HeLa cell line.** A HeLa reporter cell line expressing RFP-CWT and Lysenin^{W20A}-YFP was treated with the indicated concentrations of β-toxin and amitriptyline for 75 min, the indicated concentrations of ARC39 for 22 h, 0.5 µM PCK310 for 4h or 50/100 nM PCK310 for 22h (o.n.) and invasion efficiency of *S. aureus* JE2 was determined. (n≥5) **(D) Inhibition of ASM has no influence on the proportion of Lysenin^{W20A}-positive escape events.** The dual reporter cell line was infected with *S. aureus* JE2. Extracellular bacteria were removed and the proportion of bacteria that acquired the phagosomal escape marker RFP-CWT as well as the SM reporter Lysenin^{W20A}-YFP was determined by CLSM. The proportion of escaped (RFP-CWT-positive) bacteria that additionally acquired Lysenin^{W20A}-YFP was calculated. (n=9). **(E) ASM inhibition by amitriptyline increases phagosomal escape of *S. aureus* JE2.** The dual reporter cell line was infected with *S. aureus* JE2 and phagosomal escape rates were determined 3h p.i. (n=8). **(F) Blocking lysosomal exocytosis by Vacuolin-1 enhanced phagosomal escape.** HeLa RFP-CWT/Lysenin^{W20A}-YFP was pretreated with 1 µM Vacuolin-1 and infected with *S. aureus* JE2 for 10 min. Phagosomal escape rates were determined by CLSM 3 h p.i. (n=4). **(G) β-toxin pretreatment increases phagosomal escape of *S. aureus* JE2 but not *S. aureus* Cowan I.** RFP-CWT and Lysenin^{W20A} -YFP expressing HeLa were treated with 100 ng/ml β-toxin infected with *S. aureus* strains JE2 or Cowan I. Thereby, β-toxin was either removed prior to infection (pretreatment only) or was present during the whole experiment (pretreatment + during infection). By CLSM, proportions of bacteria that recruited RFP-CWT (phagosomal escape) were determined (n≥3). **(H) *S. aureus* strains vary in β-toxin expression.** The neutral SMase activity in culture supernatants of the indicated *S. aureus* strains or isogenic β-toxin mutants (Δ*hlb*) were determined by a TLC-based approach (n=3). **(I, J) β-toxin pretreatment of host cells but not β-toxin expression of endocytosed *S. aureus* affects phagosomal escape.** HeLa RFP-CWT/Lysenin^{W20A}-YFP were infected with *S. aureus* 6850 or an isogenic strain deficient in β-toxin production (*Δhlb*). The proportion of bacteria that escaped from the phagosome as well as the percentage of phagosomal escape events that were Lysenin^{W20A} -positive were determined 3h p.i. (n=6). **(K) Increasing the MOI compensates for shorter infection times.** HeLa cells were either infected for 10 min or 30 min with varying MOIs. Then, the number of intracellular bacteria per host cell was determined 3h p.i. by CLSM. (n=7). Statistics: Mixed effects analysis (REML) with Šídák's multiple comparison (A, G), Mixed effects analysis (REML) and Tukey's multiple comparison (I, J), One-way ANOVA with Tukey's multiple comparison (H), one samples t-test (B, C), unpaired Student's t-test (E, F). Bars represent mean +/- SD. *p≤0.05, **p≤0.01, ***p≤0.001, ****p≤0.0001.

Created with *BioRender.com/r61j266*.

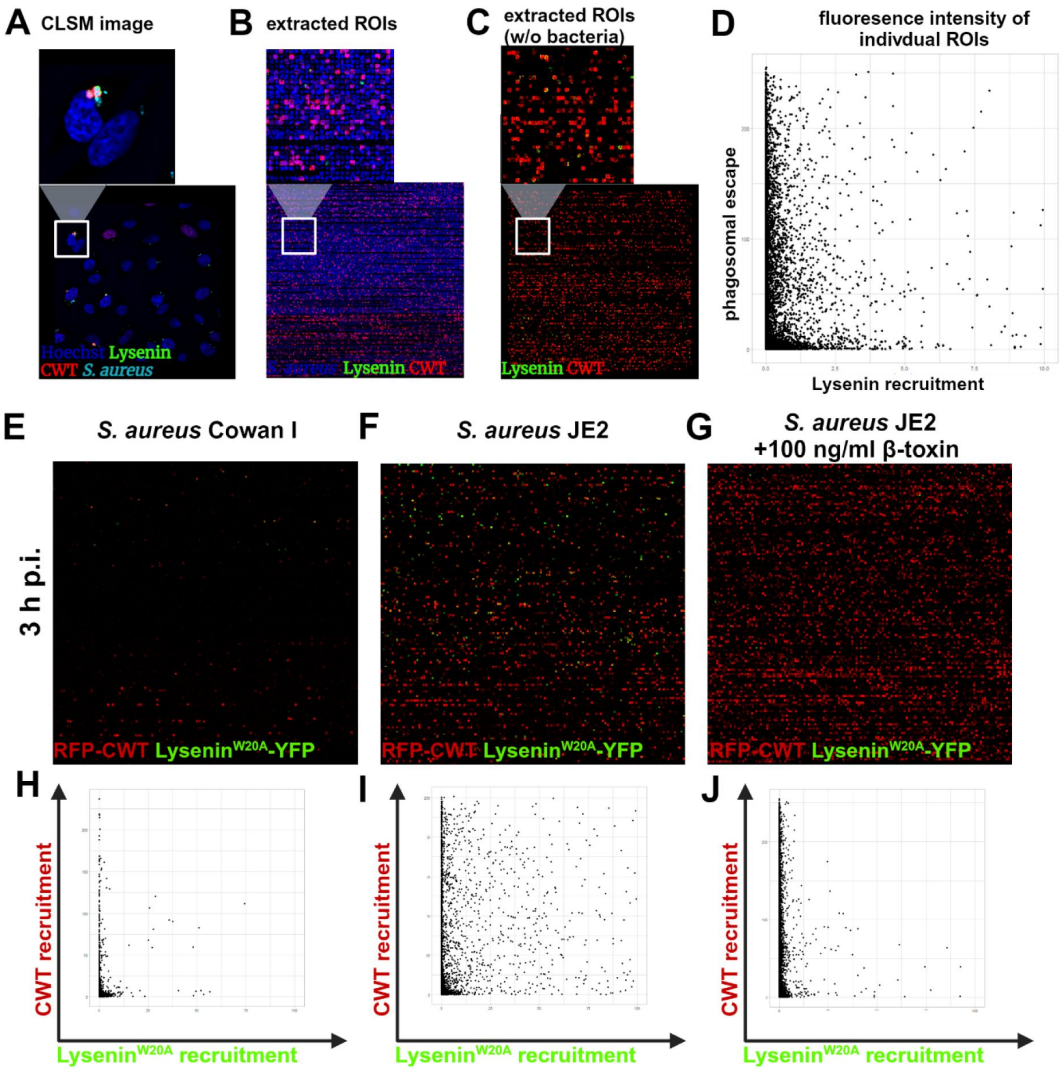

Supp. Figure 5

Evaluation of phagosomal escape and Lysenin^{W20A} recruitment during *S. aureus* infection.

HeLa reporter cells expressing RFP-CWT and Lysenin^{W20A}-YFP were infected with *S. aureus* JE2, fixed and imaged by CLSM (**A**). Individual bacteria within the images were identified as regions of interest (ROIs) and extracted in each color channel. All extracted ROIs are depicted in a montage (**B**). If bacteria signals are omitted, the montage of extracted ROIs shows the proportion of reporter recruitment. The average fluorescence intensity of both reporter fluorophores is measured within each individual ROIs is plotted as dot plots (**D**). From these results, the proportion of bacteria that recruited the markers (CWT-RFP = phagosomal escape and Lysenin^{W20A} = SM-rich-phagosome) is calculated. **(E-J) Exemplary escape assay.** Montages of extracted ROIs (without bacterial fluorescence) as well as the resulting intensity measurement in individual ROIs 3 h p.i. are depicted for infections of *S. aureus* Cowan I (E, H) and JE2 (F, I) as well as an infection with *S. aureus* JE2 in which host cells were treated with 100 ng/ml β-toxin prior to infection (G, J). Data are quantified in **Figure 4**, C.
Created with *BioRender.com/a40f830*.

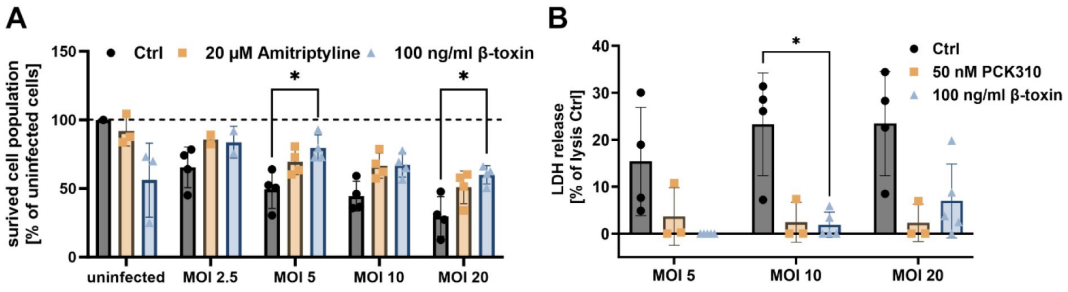

Supp. Figure 6

Inhibition of ASM and β-toxin treatment increase number of host cells remaining attached to the substratum and reduce host cell lysis during infection.

HuLEC were treated with amitriptyline or β-toxin (**A**) or PCK310 and β-toxin (**B**) and were then infected with *S. aureus* JE2. After 30 min, extracellular bacteria were removed and the number of cells remaining attached to the substratum was determined (**A**) or the proportion of host cells that were lysed during the infection was measured by lactate dehydrogenase (LDH) release (**B**). Statistics: Mixed-effects analysis and Dunnett's multiple comparison (A, B). Bars represent mean +/- SD. *p≤0.05, **p≤0.01, ***p≤0.001, ****p≤0.0001.
Created with *BioRender.com/z38g944*.

References

1. van Meer G., Voelker D. R., Feigenson G. W. (2008) **Membrane lipids: where they are and how they behave** *Nat Rev Mol Cell Biol* **9**:112–124

2. Segawa K., Suzuki J., Nagata S. (2014) **Flippases and scramblases in the plasma membrane** *Cell Cycle* **13**:2990–2991

3. Brady R. O., Kanfer J. N., Mock M. B., Fredrickson D. S. (1966) **The metabolism of sphingomyelin. II. Evidence of an enzymatic deficiency in Niemann-Pick diseae** *Proc Natl Acad Sci U S A* **55**:366–369

4. Breiden B., Sandhoff K. (2021) **Acid Sphingomyelinase, a Lysosomal and Secretory Phospholipase C, Is Key for Cellular Phospholipid Catabolism** *Int J Mol Sci* **22**

5. Li C., et al. (2018) **Regulation of Staphylococcus aureus Infection of Macrophages by CD44, Reactive Oxygen Species, and Acid Sphingomyelinase** *Antioxid Redox Signal* **28**:916–934

6. Peters S., et al. (2019) **Neisseria meningitidis Type IV Pili Trigger Ca(2+)-Dependent Lysosomal Trafficking of the Acid Sphingomyelinase To Enhance Surface Ceramide Levels** *Infect Immun* **87**

7. Grassme H., et al. (1997) **Acidic sphingomyelinase mediates entry of N. gonorrhoeae into nonphagocytic cells** *Cell* **91**:605–615

8. Fernandes M. C., et al. (2011) **Trypanosoma cruzi subverts the sphingomyelinase-mediated plasma membrane repair pathway for cell invasion** *J Exp Med* **208**:909–921

9. Carpinteiro A., et al. (2020) **Pharmacological Inhibition of Acid Sphingomyelinase Prevents Uptake of SARS-CoV-2 by Epithelial Cells** *Cell Rep Med* **1**

10. Luisoni S., et al. (2015) **Co-option of Membrane Wounding Enables Virus Penetration into Cells** *Cell Host & Microbe* **18**:75–85

11. Avota E., Gulbins E., Schneider-Schaulies S. (2011) **DC-SIGN mediated sphingomyelinase-activation and ceramide generation is essential for enhancement of viral uptake in dendritic cells** *PLoS Pathog* **7**

12. Sakr A., Brégeon F., Mège J. L., Rolain J. M., Blin O. (2018) **Staphylococcus aureus Nasal Colonization: An Update on Mechanisms, Epidemiology, Risk Factors, and Subsequent Infections** *Front Microbiol* **9**

13. McCaig L. F., McDonald L. C., Mandal S., Jernigan D. B. (2006) **Staphylococcus aureus-associated skin and soft tissue infections in ambulatory care** *Emerg Infect Dis* **12**:1715–1723

14. Liesenborghs L., et al. (2019) **Staphylococcus aureus endocarditis: distinct mechanisms of bacterial adhesion to damaged and inflamed heart valves** *Eur Heart J* **40**:3248–3259

15. Silversides J. A., Lappin E., Ferguson A. J. (2010) **Staphylococcal toxic shock syndrome: mechanisms and management** *Curr Infect Dis Rep* **12**:392–400

16. Antimicrobial Resistance C. (2022) **Global burden of bacterial antimicrobial resistance in 2019: a systematic analysis** *Lancet* **399**:629–655

17. Fraunholz M., Sinha B. (2012) **Intracellular Staphylococcus aureus: live-in and let die** *Front Cell Infect Microbiol* **2**

18. Rodrigues Lopes I., et al. (2022) **Microscopy-based phenotypic profiling of infection by Staphylococcus aureus clinical isolates reveals intracellular lifestyle as a prevalent feature** *Nature Communications* **13**

19. Hommes J. W., Surewaard B. G. J. (2022) **Intracellular Habitation of Staphylococcus aureus: Molecular Mechanisms and Prospects for Antimicrobial Therapy** *Biomedicines* **10**

20. Qazi S. N., Harrison S. E., Self T., Williams P., Hill P. J. (2004) **Real-time monitoring of intracellular Staphylococcus aureus replication** *J Bacteriol* **186**:1065–1077

21. Abel J., et al. (2011) **Staphylococcus aureus evades the extracellular antimicrobial activity of mast cells by promoting its own uptake** *J Innate Immun* **3**:495–507

22. Sinha B., et al. (1999) **Fibronectin-binding protein acts as Staphylococcus aureus invasin via fibronectin bridging to integrin alpha5beta1** *Cell Microbiol* **1**:101–117

23. Agerer F., et al. (2005) **Cellular invasion by Staphylococcus aureus reveals a functional link between focal adhesion kinase and cortactin in integrin-mediated internalisation** *J Cell Sci* **118**:2189–2200

24. Agerer F., Michel A., Ohlsen K., Hauck C. R. (2003) **Integrin-mediated invasion of Staphylococcus aureus into human cells requires Src family protein-tyrosine kinases** *J Biol Chem* **278**:42524–42531

25. Ying Y. T., et al. (2021) **Annexin A2-Mediated Internalization of Staphylococcus aureus into Bovine Mammary Epithelial Cells Requires Its Interaction with Clumping Factor B** *Microorganisms* **9**

26. Stroschein-Stevenson S. L., Foley E., O'Farrell P. H., Johnson A. D. (2006) **Identification of Drosophila gene products required for phagocytosis of Candida albicans** *PLoS Biol* **4**

27. Towell A. M., et al. (2021) **Staphylococcus aureus binds to the N-terminal region of corneodesmosin to adhere to the stratum corneum in atopic dermatitis** *Proceedings of the National Academy of Sciences* **118**

28. Askarian F., et al. (2016) **The interaction between Staphylococcus aureus SdrD and desmoglein 1 is important for adhesion to host cells** *Scientific Reports* **6**

29. Bravo-Santano N., et al. (2019) **Host-directed kinase inhibitors act as novel therapies against intracellular Staphylococcus aureus** *Scientific Reports* **9**

30. Tribelli P. M., et al. (2020) **Staphylococcus aureus Lpl protein triggers human host cell invasion via activation of Hsp90 receptor** *Cell Microbiol* **22**

31. Hirschhausen N., et al. (2010) **A novel staphylococcal internalization mechanism involves the major autolysin Atl and heat shock cognate protein Hsc70 as host cell receptor** *Cell Microbiol* **12**:1746–1764

32. Dziewanowska K., et al. (2000) **Staphylococcal fibronectin binding protein interacts with heat shock protein 60 and integrins: role in internalization by epithelial cells** *Infect Immun* **68**:6321–6328

33. Moldovan A., Fraunholz M. J. (2019) **In or out: Phagosomal escape of Staphylococcus aureus** *Cell Microbiol* **21**

34. Jauregui C. E., Mansell J. P., Jepson M. A., Jenkinson H. F. (2013) **Differential interactions of Streptococcus gordonii and Staphylococcus aureus with cultured osteoblasts** *Mol Oral Microbiol* **28**:250–266

35. Giese B., et al. (2009) **Staphylococcal alpha-toxin is not sufficient to mediate escape from phagolysosomes in upper-airway epithelial cells** *Infect Immun* **77**:3611–3625

36. Grosz M., et al. (2014) **Cytoplasmic replication of Staphylococcus aureus upon phagosomal escape triggered by phenol-soluble modulin alpha** *Cell Microbiol* **16**:451–465

37. Horn J., Stelzner K., Rudel T., Fraunholz M. (2018) **Inside job: Staphylococcus aureus host-pathogen interactions** *Int J Med Microbiol* **308**:607–624

38. Stelzner K., et al. (2021) **Intracellular Staphylococcus aureus employs the cysteine protease staphopain A to induce host cell death in epithelial cells** *PLoS Pathog* **17**

39. Gatfield J., Pieters J. (2000) **Essential role for cholesterol in entry of mycobacteria into macrophages** *Science* **288**:1647–1650

40. Zidovetzki R., Levitan I. (2007) **Use of cyclodextrins to manipulate plasma membrane cholesterol content: evidence, misconceptions and control strategies** *Biochim Biophys Acta* **1768**:1311–1324

41. Joiner K. A., Fuhrman S. A., Miettinen H. M., Kasper L. H., Mellman I. (1990) **Toxoplasma gondii: Fusion Competence of Parasitophorous Vacuoles in Fc Receptor-Transfected Fibroblasts** *Science* **249**:641–646

42. Kim S., Watarai M., Makino S.-i., Shirahata T. (2002) **Membrane sorting during swimming internalization of Brucella is required for phagosome trafficking decisions** *Microbial Pathogenesis* **33**:225–237

43. Stelzner K., et al. (2020) **Intracellular Staphylococcus aureus Perturbs the Host Cell Ca(2+) Homeostasis To Promote Cell Death** *mBio* **11**

44. Tsien R. Y. (1981) **A non-disruptive technique for loading calcium buffers and indicators into cells** *Nature* **290**:527–528

45. Krones & Rühling, et al. (2021) **Staphylococcus aureus alpha-Toxin Induces Acid Sphingomyelinase Release From a Human Endothelial Cell Line** *Front Microbiol* **12**

46. Maruyama T., Kanaji T., Nakade S., Kanno T., Mikoshiba K. (1997) **2APB, 2-aminoethoxydiphenyl borate, a membrane-penetrable modulator of Ins(1,4,5)P3-induced Ca2+ release** *J Biochem* **122**:498–505

47. Walseth T. F., Lee H. C. (1993) **Synthesis and characterization of antagonists of cyclic-ADP-ribose-induced Ca2+ release** *Biochim Biophys Acta* **1178**:235–242

48. Naylor E., et al. (2009) **Identification of a chemical probe for NAADP by virtual screening** *Nature Chemical Biology* **5**:220–226

49. Kim S. Y., Cho B. H., Kim U. H. (2010) **CD38-mediated Ca2+ signaling contributes to angiotensin II-induced activation of hepatic stellate cells: attenuation of hepatic fibrosis by CD38 ablation** *J Biol Chem* **285**:576–582

50. Rah S. Y., Mushtaq M., Nam T. S., Kim S. H., Kim U. H. (2010) **Generation of cyclic ADP-ribose and nicotinic acid adenine dinucleotide phosphate by CD38 for Ca2+ signaling in interleukin-8-treated lymphokine-activated killer cells** *J Biol Chem* **285**:21877–21887

51. Piedra-Quintero Z. L., Wilson Z., Nava P., Guerau-de-Arellano M. (2020) **CD38: An Immunomodulatory Molecule in Inflammation and Autoimmunity** *Front Immunol* **11**

52. Angeletti C., et al. (2022) **SARM1 is a multi-functional NAD(P)ase with prominent base exchange activity, all regulated bymultiple physiologically relevant NAD metabolites** *iScience* **25**

53. Rodriguez A., Webster P., Ortego J., Andrews N. W. (1997) **Lysosomes behave as Ca2+-regulated exocytic vesicles in fibroblasts and epithelial cells** *J Cell Biol* **137**:93–104

54. Cerny J., et al. (2004) **The small chemical vacuolin-1 inhibits Ca(2+)-dependent lysosomal exocytosis but not cell resealing** *EMBO Rep* **5**:883–888

55. Reddy A., Caler E. V., Andrews N. W. (2001) **Plasma membrane repair is mediated by Ca(2+)-regulated exocytosis of lysosomes** *Cell* **106**:157–169

56. Tam C., et al. (2010) **Exocytosis of acid sphingomyelinase by wounded cells promotes endocytosis and plasma membrane repair** *J Cell Biol* **189**:1027–1038

57. Roth A. G., et al. (2009) **Potent and selective inhibition of acid sphingomyelinase by bisphosphonates** *Angew Chem Int Ed Engl* **48**:7560–7563

58. Muhle C., Kornhuber J. (2017) **Assay to measure sphingomyelinase and ceramidase activities efficiently and safely** *J Chromatogr A* **1481**:137–144

59. Kappe C., Mohamed Z. H., Naser E., Carpinteiro A., Arenz C. (2020) **A Novel Visible Range FRET Probe for Monitoring Acid Sphingomyelinase Activity in Living Cells** *Chemistry* **26**:5780–5783

60. Pantůcek R., et al. (2004) **Identification of bacteriophage types and their carriage in Staphylococcus aureus** *Arch Virol* **149**:1689–1703

61. Ellison C. J., Kukulski W., Boyle K. B., Munro S., Randow F. (2020) **Transbilayer Movement of Sphingomyelin Precedes Catastrophic Breakage of Enterobacteria-Containing Vacuoles** *Curr Biol* **30**:2974–2983

62. Davis L. C., Morgan A. J., Galione A. (2020) **NAADP-regulated two-pore channels drive phagocytosis through endo-lysosomal Ca(2+) nanodomains, calcineurin and dynamin** *EMBO J* **39**

63. Sakurai Y., et al. (2015) **Ebola virus. Two-pore channels control Ebola virus host cell entry and are drug targets for disease treatment** *Science* **347**:995–998

64. Gunaratne G. S., Yang Y., Li F., Walseth T. F., Marchant J. S. (2018) **NAADP-dependent Ca(2+) signaling regulates Middle East respiratory syndrome-coronavirus pseudovirus translocation through the endolysosomal system** *Cell Calcium* **75**:30–41

65. Ou X., et al. (2020) **Characterization of spike glycoprotein of SARS-CoV-2 on virus entry and its immune cross-reactivity with SARS-CoV** *Nature Communications* **11**

66. Davis L. C., et al. (2012) **NAADP activates two-pore channels on T cell cytolytic granules to stimulate exocytosis and killing** *Curr Biol* **22**:2331–2337

67. Arredouani A., et al. (2015) **Nicotinic Acid Adenine Dinucleotide Phosphate (NAADP) and Endolysosomal Two-pore Channels Modulate Membrane Excitability and Stimulus-Secretion Coupling in Mouse Pancreatic β Cells** *J Biol Chem* **290**:21376–21392

68. Flannagan R. S., Kuiack R. C., McGavin M. J., Heinrichs D. E. (2018) **Staphylococcus aureus Uses the GraXRS Regulatory System To Sense and Adapt to the Acidified Phagolysosome in Macrophages** *mBio* **9**

69. Peng H., et al. (2015) **Acid sphingomyelinase inhibition protects mice from lung edema and lethal Staphylococcus aureus sepsis** *J Mol Med (Berl* **93**:675–689

70. Kornhuber J., et al. (2010) **Functional Inhibitors of Acid Sphingomyelinase (FIASMAs): a novel pharmacological group of drugs with broad clinical applications** *Cell Physiol Biochem* **26**:9–20

71. Kimura S., Noda T., Yoshimori T. (2007) **Dissection of the autophagosome maturation process by a novel reporter protein, tandem fluorescent-tagged LC3** *Autophagy* **3**:452–460

72. Wiznerowicz M., Trono D. (2003) **Conditional suppression of cellular genes: lentivirus vector-mediated drug-inducible RNA interference** *J Virol* **77**:8957–8961

73. Hung V., et al. (2017) **Proteomic mapping of cytosol-facing outer mitochondrial and ER membranes in living human cells by proximity biotinylation** *eLife* **6**

74. Ran F. A., et al. (2013) **Genome engineering using the CRISPR-Cas9 system** *Nature Protocols* **8**:2281–2308

75. Edgell C. J., McDonald C. C., Graham J. B. (1983) **Permanent cell line expressing human factor VIII-related antigen established by hybridization** *Proceedings of the National Academy of Sciences* **80**:3734–3737

76. Blättner S., et al. (2016) **Staphylococcus aureus Exploits a Non-ribosomal Cyclic Dipeptide to Modulate Survival within Epithelial Cells and Phagocytes** *PLOS Pathogens* **12**

77. Vann J. M., Proctor R. A. (1987) **Ingestion of Staphylococcus aureus by bovine endothelial cells results in time- and inoculum-dependent damage to endothelial cell monolayers** *Infect Immun* **55**:2155–2163

78. Fey P. D., et al. (2013) **A genetic resource for rapid and comprehensive phenotype screening of nonessential Staphylococcus aureus genes** *MBio* **4**:e00537–512

79. Becker K. A., et al. (2018) **Staphylococcus aureus Alpha-Toxin Disrupts Endothelial-Cell Tight Junctions via Acid Sphingomyelinase and Ceramide** *Infect Immun* **86**

80. Giese B., et al. (2011) **Expression of δ-toxin by Staphylococcus aureus mediates escape from phago-endosomes of human epithelial and endothelial cells in the presence of β-toxin** *Cell Microbiol* **13**:316–329

81. Schindelin J., et al. (2012) **Fiji: an open-source platform for biological-image analysis** *Nat Methods* **9**:676–682

Author information

Marcel Rühling
Chair of Microbiology, Julius-Maximilians-University Würzburg, Würzburg, Germany
ORCID iD: 0009-0006-4757-5014

Fabio Schmelz
Chair of Microbiology, Julius-Maximilians-University Würzburg, Würzburg, Germany

Kim Ulbrich
Chair of Microbiology, Julius-Maximilians-University Würzburg, Würzburg, Germany

Julia Wolf
Chair of Microbiology, Julius-Maximilians-University Würzburg, Würzburg, Germany

Maximilian Pfefferle
Chair of Microbiology, Julius-Maximilians-University Würzburg, Würzburg, Germany

Adriana Moldovan
Chair of Microbiology, Julius-Maximilians-University Würzburg, Würzburg, Germany

Nadine Knoch
Chair of Microbiology, Julius-Maximilians-University Würzburg, Würzburg, Germany

Andreas Iwanowitsch
Chair of Microbiology, Julius-Maximilians-University Würzburg, Würzburg, Germany

Christian Kappe
Institut for Chemistry, Humboldt Universität zu Berlin, Berlin, Germany

Kerstin Paprotka
Chair of Microbiology, Julius-Maximilians-University Würzburg, Würzburg, Germany

Christoph Arenz
Institut for Chemistry, Humboldt Universität zu Berlin, Berlin, Germany

Martin J Fraunholz
Chair of Microbiology, Julius-Maximilians-University Würzburg, Würzburg, Germany
ORCID iD: 0000-0002-4581-6244

For correspondence: martin.fraunholz@uni-wuerzburg.de

Editors

Reviewing Editor
Shaeri Mukherjee
University of California, San Francisco, San Francisco, United States of America

Senior Editor
Dominique Soldati-Favre
University of Geneva, Geneva, Switzerland

Reviewer #1 (Public review):

Summary:

The manuscript by Rühling et al analyzes the mode of entry of S. aureus into mammalian cells in culture. The authors propose a novel mechanism of rapid entry that involves the release of calcium from lysosomes via NAADP-stimulated activation of TPC1, which in turn causes lysosomal exocytosis; exocytic release of lysosomal acid sphingomyelinase (ASM) is then envisaged to convert exofacial sphingomyelin to ceramide. These events not only induce the rapid entry of the bacteria into the host cells but are also described to alter the fate of the intracellular S. aureus, facilitating escape from the endocytic vacuole to the cytosol.

Strengths:

The proposed mechanism is novel and could have important biological consequences.

Weaknesses:

Unfortunately, the evidence provided is unconvincing and insufficient to document the multiple, complex steps suggested. In fact, there appear to be numerous internal inconsistencies that detract from the validity of the conclusions, which were reached mostly based on the use of pharmacological agents of imperfect specificity.

Firstly, the release of calcium from lysosomes is not demonstrated. Localized changes in the immediate vicinity of lysosomes need to be measured to ascertain that these organelles are the source of cytosolic calcium changes. In fact, 9-phenantrol, which the authors find to be the most potent inhibitor of invasion and hence of the putative calcium changes, is not a blocker of lysosomal calcium release but instead blocks plasmalemmal TRPM4 channels. On the other hand, invasion is seemingly independent of external calcium. These findings are inconsistent with each other and point to non-specific effects of 9-phenantrol. The fact that ionomycin decreases invasion efficiency is taken as additional evidence of the importance of lysosomal calcium release. It is not clear how these observations support involvement of lysosomal calcium release and exocytosis; in fact treatment with the ionophore should itself have induced lysosomal exocytosis and stimulated, rather than inhibited invasion. Yet, manipulations that increase and others that decrease cytosolic calcium both inhibited invasion.

The proposed role of NAADP is based on the effects of "knocking out" TPC1 and on the pharmacological effects of Ned-19. It is noteworthy that TPC2, rather than TPC1, is generally believed to be the primary TPC isoform of lysosomes. Moreover, the gene ablation accomplished in the TPC1 "knockouts" is only partial and rather unsatisfactory. Definitive conclusions about the role of TPC1 can only be reached with proper, full knockouts. Even the pharmacological approach is unconvincing because the high doses of Ned-19 used should have blocked both TPC isoforms and presumably precluded invasion. Instead, invasion is reduced by only ≈50%. A much greater inhibition was reported using 9-phenantrol, the

blocker of plasmalemmal calcium channels. How is the selective involvement of lysosomal TPC1 channels justified?

Invoking an elevation of NAADP as the mediator of calcium release requires measurements of the changes in NAADP concentration in response to the bacteria. This was not performed. Instead, the authors analyzed the possible contribution of putative NAADP-generating systems and reported that the most active of these, CD38, was without effect, while the elimination of SARM1, another potential source of NAADP, had a very modest (≈20%) inhibitory effect that may have been due to clonal variation, which was not ruled out. In view of these data, the conclusion that NAADP is involved in the invasion process seems unwarranted.

The involvement of lysosomal secretion is, again, predicated largely on the basis of pharmacological evidence. No direct evidence is provided for the insertion of lysosomal components into the plasma membrane, or for the release of lysosomal contents to the medium. Instead, inhibition of lysosomal exocytosis by vacuolin-1 is the sole source of evidence. However, vacuolin-1 is by no means a specific inhibitor of lysosomal secretion: it is now known to act primarily as a PIKfyve inhibitor and to cause massive distortion of the endocytic compartment, including gross swelling of endolysosomes. The modest (20-25%) inhibition observed when using synaptotagmin 7 knockout cells is similarly not convincing proof of the requirement for lysosomal secretion.

ASM is proposed to play a central role in the rapid invasion process. As above, most of the evidence offered in this regard is pharmacological and often inconsistent between inhibitors or among cell types. Some drugs affect some of the cells, but not others. It is difficult to reach general conclusions regarding the role of ASM. The argument is made even more complex by the authors' use of exogenous sphingomyelinase (beta-toxin). Pretreatment with the toxin decreased invasion efficiency, a seemingly paradoxical result. Incidentally, the effectiveness of the added toxin is never quantified/validated by directly measuring the generation of ceramide or the disappearance of SM.

The use of fluorescent analogs of sphingomyelin and ceramide is not well justified and it is unclear what conclusions can be derived from these observations. Despite the low resolution of the images provided, it appears as if the labeled lipids are largely in endomembrane compartments, where they would presumably be inaccessible to the secreted ASM. Moreover, considering the location of the BODIPY probe, the authors would be unable to distinguish intact sphingomyelin from its breakdown product, ceramide. What can be concluded from these experiments? Incidentally, the authors report only 10% of BODIPY-positive events after 10 min. What are the implications of this finding? That 90% of the invasion events are unrelated to sphingomyelin, ASM, and ceramide?

It is also unclear how the authors can distinguish lysenin entry into ruptured vacuoles from the entry of RFP-CWT, used as a criterion of bacterial escape. Surely the molecular weights of the probes are not sufficiently different to prevent the latter one from traversing the permeabilized membrane until such time that the bacteria escape from the vacuole.

Both SMase inhibitors (Figure 4C) and SMase pretreatment increased bacterial escape from the vacuole. The former should prevent SM hydrolysis and formation of ceramide, while the latter treatment should have the exact opposite effects, yet the end result is the same. What can one conclude regarding the need and role of the SMase products in the escape process?

https://doi.org/10.7554/eLife.102810.1.sa2

Reviewer #2 (Public review):

Summary:

In this manuscript, Ruhling et al propose a rapid uptake pathway that is dependent on lysosomal exocytosis, lysosomal Ca2+ and acid sphingomyelinase, and further suggest that the intracellular trafficking and fate of the pathogen is dictated by the mode of entry.

The evidence provided is solid, methods used are appropriate and results largely support their conclusions, but can be substantiated further as detailed below. The weakness is a reliance on chemical inhibitors that can be non-specific to delineate critical steps.

Specific comments:

A large number of experiments rely on treatment with chemical inhibitors. While this approach is reasonable, many of the inhibitors employed such as amitriptyline and vacuolin1 have other or non-defined cellular targets and pleiotropic effects cannot be ruled out. Given the centrality of ASM for the manuscript, it will be important to replicate some key results with ASM KO cells.

Most experiments are done in HeLa cells. Given the pathway is projected as generic, it will be important to further characterize cell type specificity for the process. Some evidence for a similar mechanism in other cell types S. aureus infects, perhaps phagocytic cell type, might be good.

I'm a little confused about the role of ASM on the surface. Presumably, it converts SM to ceramide, as the final model suggests. Overexpression of b-toxin results in the near complete absence of SM on phagosomes (having representative images will help appreciate this), but why is phagosomal SM detected at high levels in untreated conditions? If bacteria are engulfed by SM-containing membrane compartments, what role does ASM play on the surface? If surface SM is necessary for phagosomal escape within the cell, do the authors imply that ASM is tuning the surface SM levels to a certain optimal range? Alternatively, can there be additional roles for ASM on the cell surface? Can surface SM levels be visualized (for example, in Figure 4 E, F)?

Related to that, why is ASM activity on the cell surface important? Its role in non-infectious or other contexts can be discussed.

If SM removal is so crucial for uptake, can exocytosis of lysosomes alone provide sufficient ASM for SM removal? How much or to what extent is lysosomal exocytosis enhanced by initial signaling events? Do the authors envisage the early events in their model happening in localized confines of the PM, this can be discussed.

How are inhibitor doses determined? How efficient is the removal of extracellular bacteria at 10 min? It will be good to substantiate the cfu experiments for infectivity with imaging-based methods. Are the roles of TPC1 and TPC2 redundant? If so, why does silencing TPC1 alone result in a decrease in infectivity? For these and other assays, it would be better to show raw values for infectivity. Please show alterations in lysosomal Ca2+ at the doses of inhibitors indicated. Is lysosomal Ca2+ released upon S. aureus binding to the cell surface? Will be good to directly visualize this.

The precise identification of cytosolic vs phagosomal bacteria is not very easy to appreciate. The methods section indicates how this distinction is made, but how do the authors deal with partial overlaps and ambiguities generally associated with such analyses? Please show respective images. The number of events (individual bacteria) for the live cell imaging data should be clearly mentioned.

In the phagosome maturation experiments, what is the proportion of bacteria in Rab5 or Rab7 compartments at each time point? Will the decreased Rab7 association be accompanied by increased Rab5? Showing raw values and images will help appreciate such differences. Given the expertise and tools available in live cell imaging, can the authors trace Rab5 and Rab7 positive compartment times for the same bacteria?

The results with longer-term infection are interesting. Live cell imaging suggests that ASM-inhibited cells show accelerated phagosomal escape that reduces by 6 hpi. Where are the bacteria at this time point ? Presumably, they should have reached lysosomes. The relationship between cytosolic escape, replication, and host cell death is interesting, but the evidence, as presented is correlative for the populations. Given the use of live cell imaging, can the authors show these events in the same cell?

Given the inherent heterogeneity in uptake processes and the use of inhibitors in most experiments, the distinction between ASM-dependent and independent pathways might not be as clear-cut as the authors suggest. Some caution here will be good. Can the authors estimate what fraction of intracellular bacteria are taken up ASM-dependent?

https://doi.org/10.7554/eLife.102810.1.sa1

Author response:

> ***Reviewer #1 (Public review):***
>
> *Summary:*
>
> *The manuscript by Rühling et al analyzes the mode of entry of S. aureus into mammalian cells in culture. The authors propose a novel mechanism of rapid entry that involves the release of calcium from lysosomes via NAADP-stimulated activation of TPC1, which in turn causes lysosomal exocytosis; exocytic release of lysosomal acid sphingomyelinase (ASM) is then envisaged to convert exofacial sphingomyelin to ceramide. These events not only induce the rapid entry of the bacteria into the host cells but are also described to alter the fate of the intracellular S. aureus, facilitating escape from the endocytic vacuole to the cytosol.*
>
> *Strengths:*
>
> *The proposed mechanism is novel and could have important biological consequences.*
>
> *Weaknesses:*
>
> *Unfortunately, the evidence provided is unconvincing and insufficient to document the multiple, complex steps suggested. In fact, there appear to be numerous internal inconsistencies that detract from the validity of the conclusions, which were reached mostly based on the use of pharmacological agents of imperfect specificity.*

We thank the reviewer for the detailed evaluation of our manuscript. We will address the criticism below.

We agree with the reviewer that many of the experiments presented in our study rely on the usage of inhibitors. However, we want to emphasize that the main conclusion (invasion pathway affects the intracellular fate/phagosomal escape) was demonstrated without the use of inhibitors or genetic ablation in two key experiments (Figure4 G/H). These experiments were in line with the results we obtained with inhibitors (amitriptyline [Supp. Figure 4E], ARC39, PCK310, [Figure 4c] and Vacuolin-1 [Supp. Figure4f]). Importantly, the hypothesis was

also supported by another key experiment, in which we showed the intracellular fate of bacteria is affected by removal of SM from the plasma membrane before invasion, but not by removal of SM from phagosomal membranes after bacteria internalization (Figure4d-f). Taken together, we thus believe that the main hypothesis is strongly supported by our data.

Moreover, we either used different inhibitors for the same molecule (ASM was inhibited by ARC39, amitriptyline and PCK310 with similar outcome) or supported our hypothesis with gene-ablated cell pools (TPC1, Syt7, SARM1), as we will point out in more detail below.

> *Firstly, the release of calcium from lysosomes is not demonstrated. Localized changes in the immediate vicinity of lysosomes need to be measured to ascertain that these organelles are the source of cytosolic calcium changes. In fact, 9-phenantrol, which the authors find to be the most potent inhibitor of invasion and hence of the putative calcium changes, is not a blocker of lysosomal calcium release but instead blocks plasmalemmal TRPM4 channels. On the other hand, invasion is seemingly independent of external calcium. These findings are inconsistent with each other and point to non-specific effects of 9-phenantrol. The fact that ionomycin decreases invasion efficiency is taken as additional evidence of the importance of lysosomal calcium release. It is not clear how these observations support involvement of lysosomal calcium release and exocytosis; in fact treatment with the ionophore should itself have induced lysosomal exocytosis and stimulated, rather than inhibited invasion. Yet, manipulations that increase and others that decrease cytosolic calcium both inhibited invasion.*

With respect to lysosomal Ca2+ release, we agree with the reviewer that direct visual demonstration of lysosomal Ca2+ release upon infection will improve the manuscript. We therefore will perform additional experimentation to show alterations of Ca2+ at the lysosomes during infection.

As to the TRPM4 involvement in *S. aureus* host cell internalization, it has been reported that TRPM4 is activated by cytosolic Ca2+. However, the channel conducts monovalent cations such as K+ or Na+ but is impermeable for Ca2+ 1, 2. The following of our observations are supporting this:

i) *S. aureus* invasion is dependent on intracellular Ca2+, but is independent from extracellular Ca2+ (Figure 1c).

ii) 9-phenantrol treatment reduces *S. aureus* internalization by host cells, illustrating the dependence of this process on TRPM4 (Figure 1b). We therefore hypothesize that TRPM4 is activated by Ca2+ released from lysosomes (see above).

TRPM4 is localized to focal adhesions and is connected to actin cytoskeleton3, 4 – a requisite of host cell entry of *S. aureus*.5, 6 This speaks for an important function of TRPM4 in uptake of *S. aureus* in general, but does not necessarily have to be involved exclusively in the *rapid uptake pathway*.

TRPM4 itself is not permeable for Ca2+ but is activated by the cation. Thus, it is unlikely to cause lysosomal exocytosis. The stronger bacterial uptake reduction by treatment with 9-phenantrol when compared to Ned19 thus may be caused by the involvement of TRPM4 in additional pathways of *S. aureus* host cell entry involving that association of TRPM4 with focal adhesions or, as pointed out by the reviewer, unspecific side effects of 9-phenantrol that we currently cannot exclude. We will include this information in the revised manuscript.

Regarding the reduced *S. aureus* invasion after ionomycin treatment, we agree with the reviewer that ionomycin is known to lead to lysosomal exocytosis as was previously shown by others7 as well as our laboratory8.

We hypothesized that pretreatment with ionomycin would trigger lysosomal exocytosis and thus would reduce the pool of lysosomes that can undergo exocytosis before host cells are contacted by *S. aureus*. As a result, we should observe a marked reduction of *S. aureus* internalization in such “lysosome-depleted cells”, if the lysosomal exocytosis is coupled to bacterial uptake. Our observation of reduced bacterial internalization after ionomycin treatment supports this hypothesis.

However, ionomycin treatment and *S. aureus* infection of host cells are distinct processes.

While ionomycin results in strong global and non-directional lysosomal exocytosis of all “releasable” lysosomes (~5-10 % of all lysosomes according to previous observations)7, we hypothesize that lysosomal exocytosis upon contact with *S. aureus* only involves a very small proportion of lysosomes at host-bacteria contact sites.

Since ionomycin disturbs the overall cellular Ca2+ homeostasis, we agree with the reviewer that this does not directly show lysosomal Ca2+ liberation. We will discuss this in more detail in the revised manuscript.

> *The proposed role of NAADP is based on the effects of "knocking out" TPC1 and on the pharmacological effects of Ned-19. It is noteworthy that TPC2, rather than TPC1, is generally believed to be the primary TPC isoform of lysosomes. Moreover, the gene ablation accomplished in the TPC1 "knockouts" is only partial and rather unsatisfactory. Definitive conclusions about the role of TPC1 can only be reached with proper, full knockouts. Even the pharmacological approach is unconvincing because the high doses of Ned-19 used should have blocked both TPC isoforms and presumably precluded invasion. Instead, invasion is reduced by only ≈50%. A much greater inhibition was reported using 9-phenantrol, the blocker of plasmalemmal calcium channels. How is the selective involvement of lysosomal TPC1 channels justified?*

As to partial gene ablation of TPC1: To avoid clonal variances, we usually perform pool sorting to obtain a cell population that predominantly contains cells -here- deficient in TPC1, but also a small proportion of wildtype cells as seen by the residual TPC1 protein on the Western blot. We observe a significant reduction of bacterial uptake in this cell pool suggesting that the uptake reduction in a pure K.O. population may be even larger.

As to the inhibition by Ned19: We agree with the reviewer that Ned19 inhibits TPC1 and TPC2. Since ablation of TPC1 reduced invasion of *S. aureus*, we concluded that TPC1 is important for *S. aureus* host cell invasion. We thus agree with the reviewer that a role for TPC2 cannot be excluded. We will clarify this in the reviewed manuscript. It needs to be noted, however, that deficiency in either TPC1 or TPC2 alone was sufficient to prevent Ebola virus infection9, which is in line with our observations.

The 50% reduction of invasion upon Ned19 treatment (Figure 1d) is comparable with the reduction caused by other compounds that influence the ASM-dependent pathway (such as amitriptyline, ARC39 [Figure 2c], BAPTA-AM [Figure 1c], Vacuolin-1 [Figure 2a], β-toxin [Figure 2e] and ionomycin [Figure 1a]). Further, the partial reduction of invasion is most likely due to the concurrent activity of multiple internalization pathways which are not all targeted by the used compounds.

> *Invoking an elevation of NAADP as the mediator of calcium release requires measurements of the changes in NAADP concentration in response to the bacteria. This was not performed. Instead, the authors analyzed the possible contribution of putative NAADP-generating systems and reported that the most active of these, CD38, was without effect, while the elimination of SARM1, another potential source of NAADP, had a very modest (≈20%) inhibitory effect that may have been due to clonal variation, which*

> *was not ruled out. In view of these data, the conclusion that NAADP is involved in the invasion process seems unwarranted.*

Our results from two independent experimental set-ups (Ned19 [Figure 1d] and TPC1 K.O. [Figure 1e & Figure 2f]) indicate the involvement of NAADP in the process. However, the measurement of NAADP concentration is non-trivial. However, we can rule out clonal variation in the SARM1 mutant since experiments were conducted with a cell pool as described above in order to avoid clonal variation of single clones.

The mechanism behind biosynthesis of NAADP is still debated. CD38 was the first enzyme discovered to possess the ability of producing NAADP. However, it requires acidic pH to produce NAADP10 -which does not match the characteristics of a cytosolic NAADP producer. HeLa cells do not express CD38 and hence, it is not surprising that inhibition of CD38 had no effect on *S. aureus* invasion in HeLa cells. However, NAADP production by HeLa cells was observed in absence of CD3811. Thus CD38-independent NAADP generation is likely. SARM1 can produce NAADP at neutral pH12 and is expressed in HeLa, thus providing a more promising candidate.

We agree with the reviewer that the reduction of *S. aureus* internalization after ablation of SARM1 is less pronounced than in other experiments of ours. This may be explained by NAADP originating from other enzymes, such as the recently discovered DUOX1, DUOX2, NOX1 and NOX213, which – with exception of DUOX2- possess a low expression even in HeLa cells. We will discuss this in the revised manuscript.

> *The involvement of lysosomal secretion is, again, predicated largely on the basis of pharmacological evidence. No direct evidence is provided for the insertion of lysosomal components into the plasma membrane, or for the release of lysosomal contents to the medium. Instead, inhibition of lysosomal exocytosis by vacuolin-1 is the sole source of evidence. However, vacuolin-1 is by no means a specific inhibitor of lysosomal secretion: it is now known to act primarily as a PIKfyve inhibitor and to cause massive distortion of the endocytic compartment, including gross swelling of endolysosomes. The modest (20-25%) inhibition observed when using synaptotagmin 7 knockout cells is similarly not convincing proof of the requirement for lysosomal secretion.*

We agree that the manuscript will strongly benefit from a functional analysis of lysosomal exocytosis. We therefore will conduct assays to investigate exocytosis in the revision. However, we previously showed i) by addition of specific antisera that LAMP1 transiently is exposed on the plasma membrane during ionomycin and pore-forming toxin challenge and ii) demonstrated the release of ASM activity into the culture medium under these conditions.8 Both measurements are not compatible with *S. aureus* infection, since LAMP1 antibodies also are non-specifically bound by protein A and another IgG-binding protein on the *S. aureus* surface, which would bias the results. Since protein A also serves as an adhesin, we cannot simply delete the ORF without changing other aspects of staphylococcal virulence. Further, FBS contains a ASM background activity that impedes activity measurements of cell culture medium. We previously removed this background activity by a specific heat-inactivation protocol.8 However, *S. aureus* invasion is strongly reduced in culture medium containing this heat-inactivated FBS.

We agree with the reviewer that Vacuolin-1 has unspecific side effects. We will address this in the revised version of the manuscript.

As to the involvement of synaptotagmin 7:

Synaptotagmin 7 is not the only protein possibly involved in Ca-dependent exocytosis. For instance, SYT1 has been shown to possess an overlapping function.14 This may explain the

discrepancy between our vacuolin-1 and SYT7 ablation experiments. We will add an according section to the discussion.

> *ASM is proposed to play a central role in the rapid invasion process. As above, most of the evidence offered in this regard is pharmacological and often inconsistent between inhibitors or among cell types. Some drugs affect some of the cells, but not others. It is difficult to reach general conclusions regarding the role of ASM. The argument is made even more complex by the authors' use of exogenous sphingomyelinase (beta-toxin). Pretreatment with the toxin decreased invasion efficiency, a seemingly paradoxical result. Incidentally, the effectiveness of the added toxin is never quantified/validated by directly measuring the generation of ceramide or the disappearance of SM.*

Although pharmacological inhibitors can have unspecific side effects, we want to emphasize that the inhibitors used in our study act on the enzyme ASM by completely different mechanisms. Amitriptyline is a so called functional inhibitor of ASM (FIASMA) which induces the detachment of ASM from lysosomal membranes resulting in degradation of the enzyme.15 By contrast, ARC39 is a competitive inhibitor.16, 17

We do not see inconsistencies in our data obtained with ASM inhibitors. Amitriptyline and ARC39 both reduce the invasion of *S. aureus* in HuLEC, HuVEC and HeLa cells (Figure 2c). ARC39 needs a longer pre-incubation, since its uptake by host cells is slower (data not shown). We observe a different outcome in 16HBE14o- and Ea.Hy 926 cells, with 16HBE14o- even demonstrating a slightly increased invasion of *S. aureus* upon ARC39 treatment. Amitriptyline had no effect (Figure 2c). Moreover, both inhibitors affected the invasion dynamics (Figure 3d), phagosomal escape (Figure 4c and Supp. Figure 4e) and Rab7 recruitment (Figure 4a and Supp. Figure 4b) in a similar fashion. Proper inhibition of ASM by both compounds in all cell lines used was validated by enzyme assays (Supp. Figure 2e), which suggests that the ASM-dependent pathway does only exist in specific cell lines. This also may serve as an argument that we here do not observe unspecific side effects of the compounds. We will clarify this in the revised manuscript.

ASM is a key player for SM degradation and recycling. In clinical context, deficiency in ASM results in the so-called Niemann Pick disease type A/B. The lipid profile of ASM-deficient cells is massively altered18, which will result in severe side effects. Short-term inhibition by small molecules therefore poses a clear benefit when compared to the usage of ASM K.O. cells.

As to the treatment with a bacterial sphingomyelinase:

Treatment with the bacterial SMase (bSMase, here: β-toxin) was performed in two different ways:

i) Pretreatment of host cells with β-toxin to remove SM from the host cell surface before infection. This removes the substrate of ASM from the cell surface prior to addition of the bacteria (Figure 2e, Figure 4d-f). Since SM is not present on the extracellular plasma membrane leaflet after treatment, a release of ASM cannot cause localized ceramide formation at the sites of lysosomal exocytosis. Similar observations were made by others.19

ii) Addition of bSMase to host cells together with the bacteria to complement for the absence of ASM (Figure 2f).

Removal of the ASM substrate before infection (i) prevents localized ASM-mediated conversion of SM to Cer during infection and resulted in a decreased invasion, while addition of the SMase during infection resulted in an increased invasion in TPC1 and SYT7 ablated cells. Thus, both experiments are consistent with each other and in line with our other observations.

Removal of SM from the plasma membrane by β-toxin was indirectly demonstrated by the absence of Lysenin recruitment to phagosomes/escaped bacteria when host cells were pretreatment with the toxin before infection (Figure4F). In another publication, we recently quantified the effectiveness of β-toxin treatment, even though with slightly longer treatment times (75 min vs. 3h).20 We will repeat the measurements also for shorter treatment times.

To clarify our experimental approaches to the readership we will add an explanatory section to the revised manuscript.

As to the general conclusions regarding the role of ASM: ASM and lysosomal exocytosis has been shown to be involved in uptake of a variety of pathogens19, 21-25 supporting its role in the process.

> *The use of fluorescent analogs of sphingomyelin and ceramide is not well justified and it is unclear what conclusions can be derived from these observations. Despite the low resolution of the images provided, it appears as if the labeled lipids are largely in endomembrane compartments, where they would presumably be inaccessible to the secreted ASM. Moreover, considering the location of the BODIPY probe, the authors would be unable to distinguish intact sphingomyelin from its breakdown product, ceramide. What can be concluded from these experiments? Incidentally, the authors report only 10% of BODIPY-positive events after 10 min. What are the implications of this finding? That 90% of the invasion events are unrelated to sphingomyelin, ASM, and ceramide?*

During the experiments with fluorescent SM analogues (Figure 3a,b), *S. aureus* was added to the samples immediately before start of video recording. Hence, bacteria are slowly trickling onto the host cells and we thus can image the initial contact between them and the bacteria, for instance, the bacteria depicted in Figure 3a contact the host cell about 9 min before becoming BODIPY-FL-positive (see Supp. Video 1, 55 min). Hence, we think that in these cases we see the formation of phagosomes around bacteria rather than bacteria in endomembrane compartments. Since generation of phagosomes happens at the plasma membrane, SM is accessible to secreted ASM.

The “trickling” approach for infection is an experimental difference to our invasion measurements, in which we synchronized the infection by a very slow centrifugation. This ensures that all bacteria have contact to host cells and are not just floating in the culture medium. However, live cell imaging of initial bacterial-host contact and synchronization of infection is technically not combinable.

In our invasion measurements -with synchronization-, we typically see internalization of ~20% of all added bacteria after 30 min. Hence, most bacteria that are visible in our videos likely are still extracellular and only a small proportion was internalized. This explains why only 10% of total bacteria are positive for BODIPY-FL-SM after 10 min. The proportion of internalized bacteria that are positive for BODIPY-FL-SM should be way higher but cannot be determined with this method.

We agree with the reviewer that we cannot observe conversion of BODIPY-FL-SM by ASM. In order to do that, we attempted to visualize the conversion of a visible-range SM FRET probe (Supp. Figure 3), but the structure of the probe is not compatible with measurement of conversion on the plasma membrane, since the FITC fluorophore released into the culture medium by the ASM activity thereby gets lost for imaging. In general, the visualization of SM conversion with subcellular resolution is challenging and even with novel tools developed in our lab26 visualization of SM on the plasma membrane is difficult.

The conclusion we draw from these experiments are that i.) *S. aureus* invasion is associated with SM and ii.) SM-associated invasion can be very fast, since bacteria are rapidly engulfed by BODIPY-FL-SM containing membranes.

> *It is also unclear how the authors can distinguish lysenin entry into ruptured vacuoles from the entry of RFP-CWT, used as a criterion of bacterial escape. Surely the molecular weights of the probes are not sufficiently different to prevent the latter one from traversing the permeabilized membrane until such time that the bacteria escape from the vacuole.*

We here want to clarify that both, the Lysenin as well as the CWT reporter have access to rupture vacuoles (Figure 4b). We used the Lysenin reporter in these experiments for estimation of SM content of phagosomal membranes. If a vacuole is ruptured, both the bacteria and the luminal leaflet of the phagosomal membrane remnants get in contact with the cytosol and hence with the cytosolically expressed reporters YFP-Lysenin as well as RFP-CWT resulting in “Lysenin-positive escape” when phagosomes contained SM (see Figure 4f). By contrast, either β-toxin expression by S. aureus or pre-treatment with the bSMase resulted in absence of Lysenin recruitment suggesting that the phagosomal SM levels were decreased/undetectable (Figure 4f, Supp Figure 5f, g, i, j).

This approach does not enable a quantitative measurement of phagosomal SM and rather gives a “yes or no” answer. However, we think this method is sufficient to show that β-toxin expression and pretreatment markedly decreased phagosomal SM levels in the host cells.

The approach we used here to analyze “Lysenin-positive escape” can clearly be distinguished from Lysenin-based methods that were used by others.27 There Lysenin was used to show trans-bilayer movement of SM before rupture of bacteria-containing phagosomes.

To clarify the function of Lysenin in our approach we will add an additional figure to the revised manuscript.

> *Both SMase inhibitors (Figure 4C) and SMase pretreatment increased bacterial escape from the vacuole. The former should prevent SM hydrolysis and formation of ceramide, while the latter treatment should have the exact opposite effects, yet the end result is the same. What can one conclude regarding the need and role of the SMase products in the escape process?*

As pointed out above, pretreatment of host cells with SMase removes SM from the plasma membrane and hence, ASM does not have access to its substrate. Hence, both treatment with either ASM inhibitors or pretreatment with bacterial SMase prevent ASM from being active on the plasma membrane and hence block the ASM-dependent uptake (Figure 2 c, e). Although overall less bacteria were internalized by host cells under these conditions, the bacteria that invaded host cells did so in an ASM-independent manner.

Since blockage of the ASM-dependent internalization pathway (with ASM inhibitor [Figure 4c], SMase pretreatment [Figure 4e] and Vacuolin-1[Supp. Fig.4f]) always resulted in enhanced phagosomal escape, we conclude that bacteria that were internalized in an ASM-independent fashion cause enhanced escape. Vice versa, bacteria that enter host cells in an ASM-dependent manner demonstrate lower escape rates.

This is supported by comparing the escape rates of “early” and “late” invaders [Figure 4g/h], which in our opinion is a key experiment that supports this hypothesis. The “early” invaders are predominantly ASM-dependent (see e.g. Figure 3e) and thus, bacteria that entered host cell in the first 10 min of infection should have been internalized predominantly in an ASM-dependent fashion, while slower entry pathways are active later during infection. The early

ASM dependent invaders possessed lower escape rates, which is in line with the data obtained with inhibitors (e.g. Figure 4c and Supp. Fig. 4f).

We hypothesize that the activity of ASM on the plasma membrane during invasion mediates the recruitment of a specific subset of receptors, which then influence downstream phagosomal maturation and escape. This hypothesis is supported by the fact that the subset of receptors interacting with *S. aureus* is altered upon inhibition of the ASM-dependent uptake pathway. We describe this in another study that is currently under evaluation elsewhere.

> ***Reviewer #2 (Public review):***
>
> *Summary:*
>
> *In this manuscript, Ruhling et al propose a rapid uptake pathway that is dependent on lysosomal exocytosis, lysosomal Ca2+ and acid sphingomyelinase, and further suggest that the intracellular trafficking and fate of the pathogen is dictated by the mode of entry.*
>
> *The evidence provided is solid, methods used are appropriate and results largely support their conclusions, but can be substantiated further as detailed below. The weakness is a reliance on chemical inhibitors that can be non-specific to delineate critical steps.*
>
> *Specific comments:*
>
> *A large number of experiments rely on treatment with chemical inhibitors. While this approach is reasonable, many of the inhibitors employed such as amitriptyline and vacuolin1 have other or non-defined cellular targets and pleiotropic effects cannot be ruled out. Given the centrality of ASM for the manuscript, it will be important to replicate some key results with ASM KO cells.*

We thank the reviewer for the critical evaluation of our manuscript and plenty of constructive comments.

We agree with the reviewer, that ASM inhibitors such as functional inhibitors of ASM (FIASMA) like amitriptyline used in our study have unspecific side effects given their mode-of-action. FIASMAs induce the detachment of ASM from lysosomal membranes resulting in degradation of the enzyme.15 However, we want to emphasize that we also used the competitive inhibitor ARC39 in our study16, 17 which acts on the enzyme by a completely different mechanism. All phenotypes (reduced invasion [Figure 2c, d], effect on invasion dynamics [Figure 3d], enhanced escape [Figure 4c and Supp Figure 4e] and differential recruitment of Rab7 [Supp. Figure 4b]) were observed with both inhibitors thereby supporting the role of ASM in the process.

We further agree that experiments with genetic evidence usually support and improve scientific findings. However, ASM is a cellular key player for SM degradation and recycling. In a clinical context, deficiency in ASM results in a so-called Niemann Pick disease type A/B. The lipid profile of ASM-deficient cells is massively altered18, which in itself will result in severe side effects. Thus, the usage of inhibitors provides a clear benefit when compared to ASM K.O. cells, since ASM activity can be targeted in a short-term fashion thereby preventing larger alterations in cellular lipid composition.

> *Most experiments are done in HeLa cells. Given the pathway is projected as generic, it will be important to further characterize cell type specificity for the process. Some evidence for a similar mechanism in other cell types S. aureus infects, perhaps phagocytic cell type, might be good.*

Whenever possible we performed the experiments not only in HeLa but also in HuLECs. For example, we refer to experiments concerning the role of Ca2+ (Figure 1c/Supp.Figure1e), lysosomal Ca2+/Ned19 (Figure1d/Supp Figure 1g), lysosomal exocytosis/Vacuolin-1 (Figure 2a/Supp. Figure2a), ASM/ARC39 and amitriptyline (Figure 2c), surface SM/β-toxin (Figure 2e/Supp. Figure 2g), analysis of invasion dynamics (complete Figure 3) and measurement of cell death during infection (Figure 5c-e, Supp. Figure 6a+b).

HuLECs, however, are not really genetically amenable and hence we were not able to generate gene deletions in these cells and upon introduction of the fluorescence escape reporter the cells are not readily growing.

As to ASM involvement in phagocytic cells: a role for ASM during the uptake of *S. aureus* by macrophages was previously reported by others.23 However, in professional phagocytes *S. aureus* does not escape from the phagosome and replicates within the vacuole.28

> *I'm a little confused about the role of ASM on the surface. Presumably, it converts SM to ceramide, as the final model suggests. Overexpression of b-toxin results in the near complete absence of SM on phagosomes (having representative images will help appreciate this), but why is phagosomal SM detected at high levels in untreated conditions? If bacteria are engulfed by SM-containing membrane compartments, what role does ASM play on the surface? If surface SM is necessary for phagosomal escape within the cell, do the authors imply that ASM is tuning the surface SM levels to a certain optimal range? Alternatively, can there be additional roles for ASM on the cell surface? Can surface SM levels be visualized (for example, in Figure 4 E, F)?*

We initially hypothesized that we would detect higher phagosomal SM levels upon inhibition of ASM, since our model suggests SM cleavage by ASM on the host cell surface during bacterial cell entry. However, we did not detect any changes in our experiments (Supp. Figure 4d). We currently favor the following explanation: SM is the most abundant sphingolipid in human cells.29 If peripheral lysosomes are exocytosed and thereby release ASM, only a localized and relative small proportion of SM may get converted to Cer, which most likely is below our detection limit. In addition, the detection of cytosolically exposed phagosomal SM by YFP-Lysenin is not quantitative and provides a “Yes or No” measurement. Hence, we think that the rather limited SM to Cer conversion in combination with the high abundance of SM in cellular membranes does not visibly affect the recruitment of the Lysenin reporter.

In our experiments that employ BODIPY-FL-SM (Figure 3a+b), we cannot distinguish between native SM and downstream metabolites such as Cer. Hence, again we cannot make any assumptions on the extent to which SM is converted on the surface during bacterial internalization. Although our laboratory recently used trifunctional sphingolipid analogs to analyze the SM to Cer conversion20, the visualization of this process on the plasma membrane is currently still challenging.

Overall, we hypothesize that the localized generation of Cer on the surface by released ASM leads to generation of Cer-enriched platforms. Subsequently, a certain subset of receptors may be recruited to these platforms and influence the uptake process. These platforms are supposed to be very small, which also would explain that we did not detect changes in Lysenin recruitment.

> *Related to that, why is ASM activity on the cell surface important? Its role in non-infectious or other contexts can be discussed.*

ASM release by lysosomal exocytosis is implied in plasma membrane repair upon injury. We will this discuss this in the revised version of the manuscript.

> *If SM removal is so crucial for uptake, can exocytosis of lysosomes alone provide sufficient ASM for SM removal? How much or to what extent is lysosomal exocytosis enhanced by initial signaling events? Do the authors envisage the early events in their model happening in localized confines of the PM, this can be discussed.*

Ionomycin treatment led to a release of ~10 % of all lysosomes and also increased extracellular ASM activity.7, 8 However, it is currently unclear– to our knowledge -to which extent the released ASM affects surface SM levels. Also, it is unknown which percentage of the lysosomes is released during infection with *S. aureus*. However, one has to speculate that this will be only a fraction of the "releasable lysosomes" as we assume that the effects (lysosomal Ca2+ liberation, lysosomal exocytosis and ASM activity) are very localized and take place only at host-pathogen contact sites (see also above). In initial experimentation we attempted to visualize the local ASM activity on the cell surface by using a visible range FRET probe (Supp. Fig. 3). Cleavage of the probe by ASM on the surface leads to release of FITC into the cell culture medium which does not contribute a measurable signal at the surface.

> *How are inhibitor doses determined? How efficient is the removal of extracellular bacteria at 10 min? It will be good to substantiate the cfu experiments for infectivity with imaging-based methods. Are the roles of TPC1 and TPC2 redundant? If so, why does silencing TPC1 alone result in a decrease in infectivity? For these and other assays, it would be better to show raw values for infectivity. Please show alterations in lysosomal Ca2+ at the doses of inhibitors indicated. Is lysosomal Ca2+ released upon S. aureus binding to the cell surface? Will be good to directly visualize this.*

Concerning the inhibitor concentrations, we either used values established in published studies or recommendations of the suppliers (e.g. 2-APB, Ned19, Vacuolin-1). For ASM inhibitors, we determined proper inhibition of ASM by activity assays. Concentrations of ionomycin resulting in Ca2+ influx and lysosomal exocytosis was determined in earlier studies of our lab.8, 30

As to the removal of bacteria at 10 min p.i.: Lysostaphin is very efficient for removal of extracellular *S. aureus* and sterilizes the tissue culture supernatant. It significantly lyses bacteria within a few minutes, as determined by turbidity assays.31

As to imaging-based infectivity assays: We will add an analysis of imaging-based invasion assays in the revised manuscript.

Regarding the roles of TPC1 and TPC2: from our data we cannot conclude whether the roles of TPC1 and TPC2 are redundant. One could speculate that since blockage of TPC1 alone is sufficient to reduce internalization of bacteria, that both channels may have distinct roles. On the other hand, there might be a Ca2+ threshold in order to initiate lysosomal exocytosis that can only be attained if TPC1 and TPC2 are activated in parallel. Thus, our observations are in line with another study that shows reduced Ebola virus infection in absence of either TPC1 or TPC2.32

As to raw CFU counts: whereas the observed effects upon blocking the invasion of *S. aureus* are stable, the number of internalized bacteria varies between individual biological replicates, for instance, by differences in host cell fitness or growth differences in bacterial cultures, which are prepared freshly for each experiment.

With respect to visualization of lysosomal Ca2+ release: we agree with the reviewer that direct visual demonstration of lysosomal Ca2+ release upon infection will improve the manuscript. We therefore will perform additional experimentation to show alterations of Ca2+ at the lysosomes during infection.

> *The precise identification of cytosolic vs phagosomal bacteria is not very easy to appreciate. The methods section indicates how this distinction is made, but how do the authors deal with partial overlaps and ambiguities generally associated with such analyses? Please show respective images. The number of events (individual bacteria) for the live cell imaging data should be clearly mentioned.*

We apologize for not having sufficiently explained the technology to detect escaped *S. aureus*. The cytosolic location of *S. aureus* is indicated by recruitment of RFP-CWT.33 CWT is the cell wall targeting domain of lysostaphin, which efficiently binds to the pentaglycine cross bridge in the peptidoglycan of *S. aureus*. This reporter is exclusively and homogenously expressed in the host cytosol. Only upon rupture of phagoendosomal membranes the reporter can be recruited to the cell wall of now cytosolically located bacteria. *S. aureus* mutants, for instance in the agr quorum sensing system, cannot break down the phagosomal membrane in non-professional phagocytes and thus stay unlabeled by the CWT-reporter.33 We will include respective images/movies of escape events and the bacteria numbers for live cell experiments in the revised version of the manuscript.

> *In the phagosome maturation experiments, what is the proportion of bacteria in Rab5 or Rab7 compartments at each time point? Will the decreased Rab7 association be accompanied by increased Rab5? Showing raw values and images will help appreciate such differences. Given the expertise and tools available in live cell imaging, can the authors trace Rab5 and Rab7 positive compartment times for the same bacteria?*

We will include the proportion of Rab7-associated bacteria in the revised manuscript. Usually, we observe that Rab5 is only transiently (for a few minutes) present on phagosomes and only afterwards the phagosomes become positive for Rab7. We do not think that a decrease in Rab7-positive phagosomes would increase the proportion of Rab5-positive phagosomes. However, we cannot exclude this hypothesis with our data.

We can achieve tracing of individual bacteria for recruitment of Rab5/Rab7 only manually, which impedes a quantitative evaluation. However, we will include information that illustrates the consecutive recruitment of the GTPases.

> *The results with longer-term infection are interesting. Live cell imaging suggests that ASM-inhibited cells show accelerated phagosomal escape that reduces by 6 hpi. Where are the bacteria at this time point ? Presumably, they should have reached lysosomes. The relationship between cytosolic escape, replication, and host cell death is interesting, but the evidence, as presented is correlative for the populations. Given the use of live cell imaging, can the authors show these events in the same cell?*

We think that most bacteria-containing phagoendosomes should have fused with lysosomes 6 h p.i. as we have previously shown by acidification to pH of 5 and LAMP1 decoration.34

We will provide images/videos to show the correlation between escape and replication in the revised manuscript.

> *Given the inherent heterogeneity in uptake processes and the use of inhibitors in most experiments, the distinction between ASM-dependent and independent pathways might not be as clear-cut as the authors suggest. Some caution here will be good. Can the authors estimate what fraction of intracellular bacteria are taken up ASM-dependent?*

We agree with the reviewer that an overlap between internalization pathways is likely. A clear distinction is therefore certainly non-trivial. Alternative to ASM-dependent and ASM-

independent pathways, the ASM activity may also accelerate one or several internalization pathways. We will address this limitation in the revised manuscript.

Early in infection (~10 min after contact with the cells), the proportion of bacteria that enter host cells ASM-dependently is relatively high amounting to roughly 75% in HuLEC. After 30 min, this proportion is decreasing to about 50%. We will include this information in the revised version of the manuscript.

References

(1) Launay, P. et al. TRPM4 Is a Ca2+-Activated Nonselective Cation Channel Mediating Cell Membrane Depolarization. *Cell* 109, 397-407 (2002).

(2) Nilius, B. et al. The Ca^{2+}-activated cation channel TRPM4 is regulated by phosphatidylinositol 4,5-biphosphate. *The EMBO Journal* 25, 467-478-478 (2006).

(3) Cáceres, M. et al. TRPM4 Is a Novel Component of the Adhesome Required for Focal Adhesion Disassembly, Migration and Contractility. *PLoS One* 10, e0130540 (2015).

(4) Silva, I., Brunett, M., Cáceres, M. & Cerda, O. TRPM4 modulates focal adhesion-associated calcium signals and dynamics. *Biophysical Journal* 123, 390a (2024).

(5) Schlesier, T., Siegmund, A., Rescher, U. & Heilmann, C. Characterization of the Atl-mediated staphylococcal internalization mechanism. *International Journal of Medical Microbiology* 310, 151463 (2020).

(6) Jevon, M. et al. Mechanisms of Internalization ofStaphylococcus aureus by Cultured Human Osteoblasts. *Infection and Immunity* 67, 2677-2681 (1999).

(7) Rodriguez, A., Webster, P., Ortego, J. & Andrews, N.W. Lysosomes behave as Ca2+-regulated exocytic vesicles in fibroblasts and epithelial cells. *J Cell Biol* 137, 93-104 (1997).

(8) Krones & Rühling et al. Staphylococcus aureus alpha-Toxin Induces Acid Sphingomyelinase Release From a Human Endothelial Cell Line. *Front Microbiol* 12, 694489 (2021).

(9) Sakurai, Y. et al. Two-pore channels control Ebola virus host cell entry and are drug targets for disease treatment. *Science* 347, 995-998 (2015).

(10) Aarhus, R., Graeff, R.M., Dickey, D.M., Walseth, T.F. & Lee, H.C. ADP-ribosyl cyclase and CD38 catalyze the synthesis of a calcium-mobilizing metabolite from NADP. *J Biol Chem* 270, 30327-30333 (1995).

(11) Schmid, F., Fliegert, R., Westphal, T., Bauche, A. & Guse, A.H. Nicotinic acid adenine dinucleotide phosphate (NAADP) degradation by alkaline phosphatase. *J Biol Chem* 287, 32525-32534 (2012).

(12) Angeletti, C. et al. SARM1 is a multi-functional NAD(P)ase with prominent base exchange activity, all regulated bymultiple physiologically relevant NAD metabolites. *iScience* 25, 103812 (2022).

(13) Gu, F. et al. Dual NADPH oxidases DUOX1 and DUOX2 synthesize NAADP and are necessary for Ca(2+) signaling during T cell activation. *Sci Signal* 14, eabe3800 (2021).

(14) Schonn, J.-S., Maximov, A., Lao, Y., Südhof, T.C. & Sørensen, J.B. Synaptotagmin-1 and -7 are functionally overlapping Ca^{2+} sensors for exocytosis in adrenal chromaffin cells. *Proceedings of the National Academy of Sciences* 105, 3998-4003 (2008).

(15) Kornhuber, J. et al. Functional Inhibitors of Acid Sphingomyelinase (FIASMAs): a novel pharmacological group of drugs with broad clinical applications. *Cell Physiol Biochem* 26, 9-20 (2010).

(16) Naser, E. et al. Characterization of the small molecule ARC39, a direct and specific inhibitor of acid sphingomyelinase in vitro. *J Lipid Res* 61, 896-910 (2020).

(17) Roth, A.G. et al. Potent and selective inhibition of acid sphingomyelinase by bisphosphonates. *Angew Chem Int Ed Engl* 48, 7560-7563 (2009).

(18) Schuchman, E.H. & Desnick, R.J. Types A and B Niemann-Pick disease. *Mol Genet Metab* 120, 27-33 (2017).

(19) Miller, M.E., Adhikary, S., Kolokoltsov, A.A. & Davey, R.A. Ebolavirus Requires Acid Sphingomyelinase Activity and Plasma Membrane Sphingomyelin for Infection. *Journal of Virology* 86, 7473-7483 (2012).

(20) M. Rühling, L.K., F. Wagner, F. Schumacher, D. Wigger, D. A. Helmerich, T. Pfeuffer, R. Elflein, C. Kappe, M. Sauer, C. Arenz, B. Kleuser, T. Rudel, M. Fraunholz, J. Seibel Trifunctional sphingomyelin derivatives enable nanoscale resolution of sphingomyelin turnover in physiological and infection processes via expansion microscopy. *Nat Commun* accepted in principle (2024).

(21) Peters, S. et al. Neisseria meningitidis Type IV Pili Trigger Ca(2+)-Dependent Lysosomal Trafficking of the Acid Sphingomyelinase To Enhance Surface Ceramide Levels. *Infect Immun* 87 (2019).

(22) Grassmé, H. et al. Acidic sphingomyelinase mediates entry of N. gonorrhoeae into nonphagocytic cells. *Cell* 91, 605-615 (1997).

(23) Li, C. et al. Regulation of Staphylococcus aureus Infection of Macrophages by CD44, Reactive Oxygen Species, and Acid Sphingomyelinase. *Antioxid Redox Signal* 28, 916-934 (2018).

(24) Fernandes, M.C. et al. Trypanosoma cruzi subverts the sphingomyelinase-mediated plasma membrane repair pathway for cell invasion. *J Exp Med* 208, 909-921 (2011).

(25) Luisoni, S. et al. Co-option of Membrane Wounding Enables Virus Penetration into Cells. *Cell Host & Microbe* 18, 75-85 (2015).

(26) Rühling, M. et al. Trifunctional sphingomyelin derivatives enable nanoscale resolution of sphingomyelin turnover in physiological and infection processes via expansion microscopy. *Nature Communications* 15, 7456 (2024).

(27) Ellison, C.J., Kukulski, W., Boyle, K.B., Munro, S. & Randow, F. Transbilayer Movement of Sphingomyelin Precedes Catastrophic Breakage of Enterobacteria-Containing Vacuoles. *Curr Biol* 30, 2974-2983 e2976 (2020).

(28) Moldovan, A. & Fraunholz, M.J. In or out: Phagosomal escape of Staphylococcus aureus. *Cell Microbiol* 21, e12997 (2019).

(29) Slotte, J.P. Biological functions of sphingomyelins. *Progress in Lipid Research* 52, 424-437 (2013).

(30) Stelzner, K. et al. Intracellular Staphylococcus aureus Perturbs the Host Cell Ca(2+) Homeostasis To Promote Cell Death. *mBio* 11 (2020).

(31) Kunz, T.C. et al. The Expandables: Cracking the Staphylococcal Cell Wall for Expansion Microscopy. *Front Cell Infect Microbiol* 11, 644750 (2021).

(32) Sakurai, Y. et al. Ebola virus. Two-pore channels control Ebola virus host cell entry and are drug targets for disease treatment. *Science* 347, 995-998 (2015).

(33) Grosz, M. et al. Cytoplasmic replication of Staphylococcus aureus upon phagosomal escape triggered by phenol-soluble modulin alpha. *Cell Microbiol* 16, 451-465 (2014).

(34) Giese, B. et al. Staphylococcal alpha-toxin is not sufficient to mediate escape from phagolysosomes in upper-airway epithelial cells. *Infect Immun* 77, 3611-3625 (2009).

https://doi.org/10.7554/eLife.102810.1.sa0